

ANALYSIS AND INTERPRETATION OF ICE-DEFORMED  
SEDIMENTS FROM HARRISON BAY, ALASKA

By  
Steven A. Fischbein<sup>1</sup>

Open-File Report 87-262

This report was prepared under contract to the U.S. Geological Survey and has not been reviewed for conformity with USGS editorial standards and stratigraphic nomenclature. Opinions and conclusions expressed herein do not necessarily represent those of the USGS.

<sup>1</sup>Geology Department, California State University, Hayward, CA

## CONTENT

	Page
Abstract.....	1
Acknowledgements.....	1
Introduction.....	2
Location and Geologic Setting.....	2
Previous Work.....	3
Purpose of Investigation.....	3
Method of Study.....	3
Core Examination Procedure.....	7
General Geology	
The Coastal Plain.....	7
The Shelf.....	8
General Core Descriptions and Environments of Deposition..	11
Discussion	
Environments of Deposition.....	11
Ice Related Deformation.....	38
Ice Sediment Interaction.....	41
Glacial Lake Agassiz:	
An Example of Preserved Ice Gouges.....	48
Late Pleistocene Lacustrine Sediments of the Ontario Basin, Canada: An Alternative Interpretation.....	51
Summary.....	54
Conclusions.....	54
Appendix A.....	55
References Cited.....	69

FIGURES

	Page
Figure 1a. General Locality Map.....	3
Figure 1b. Detailed Locality Map.....	4
Figure 2. Side Scan Sonar Image.....	5
Figure 3a. Uniboom Seismic Profile.....	9
Figure 3b. 7 Khz and 200 Khz Seismic Profile.....	10
Figure 4a and b. Core V-13.....	13
Figure 5a and b. Core V-14.....	15
Figure 6a and b. Core V-15.....	16
Figure 7a and b. Core V-16.....	18
Figure 8a and b. Core V-17.....	19
Figure 9a and b. Core V-18.....	20
Figure 10a and b. Core V-19.....	22
Figure 11a and b. Core V-20.....	23
Figure 12a and b. Core V-21.....	25
Figure 13a and b. Core V-22.....	26
Figure 14a and b. Core V-23.....	27
Figure 15a and b. Core V-53.....	29
Figure 16a and b. Core V-55.....	30
Figure 17. Core V-76.....	32
Figure 18a. Comparison Cores from Guadalupe Delta.....	35
Figure 18b. Comparison Cores from Guadalupe Delta.....	36
Figure 19. Shelf Profile and Facies Associations.....	37
Figure 20a, b, c. Ice Gouge Deformation Model.....	39
Figure 21. Schematic Drawing of Ice Gouge Process.....	42

Figure 22. Hypothetical Cross-Section.....	43
Figure 23. Sketch of Core V-16.....	44
Figure 24. North Sea Ice-Deformed Sediments.....	45
Figure 25. Ice Gouge Intensity Map.....	46
Figure 26. Ice Gouged Sediments From Lake Agassiz.....	50
Figure 27. Ice Gouged Sediments From Lake Ontario.....	52

## ABSTRACT

The surficial sediments present on the continental shelf off the north coast of Alaska in the vicinity of Harrison Bay consist dominantly of fine grained sand, silt, and mud that were deposited during Holocene time. Depositional environments in Harrison Bay range from outer shelf to prodelta and delta front.

Ice sediment interaction has overprinted structural deformation on many of the sediments present in Harrison Bay, and has in some cases obliterated the original lithologic continuity of the sediments. Ice related deformation ranges from simple loading features to more complex folded and faulted structures. A hypothetical model has been proposed which relates the type of deformational features found in recent sediments from an ice impacted area to the process of ice gouging.

The deformational structures observed in the sediments from Harrison Bay were compared to deformational features found in sediments from ancient environments that are known to have had floating ice present. The results indicate that structures found in the modern environment bear a remarkable similarity to structures found in the ancient environments, and that the structures found in the ancient environments are believed to have been caused by the process of ice gouging.

## ACKNOWLEDGEMENTS

I would like to thank Dr. Detlef Warnke for offering me the chance to work on this project and managing all the administrative details associated with it. I would also like to thank Dr. Peter Barnes and Dr. Erk Reimnitz of the United States Geological Survey for allocating the funding for this project, critically reviewing the manuscript, and allowing me to analyze their field data. I also offer thanks to Mr. Mike Zani for helping me understand the math behind the physics of partially buoyant objects.

I offer my most sincere thanks and gratitude to my parents, Irwin and Sarah Fischbein, whose love and undying belief in my ability has always motivated me to pursue ever higher education, and to my wife Robin, who has supported me both financially and emotionally through this degree and who has constantly encouraged me to chase my second greatest love only to her, geology.

Finally I would like to dedicate this work in memorium to Dr. Geoffrey Davidson Woodard whose lust for the science of geology was contagious and inspirational, and who, in the face of terminal cancer, threw down the gauntlet to the powers that be and continued his field

work to the end.

## INTRODUCTION

Depositional processes on high latitude continental shelves are obscured by the presence of pack ice for at least three-fourths of every year. The role which the ice plays in influencing the sediment deposited on the continental shelf is not yet fully understood, although many ideas have been formulated. One ice-sediment interactive process known to occur is that of ice gouging or ice ploughing. The internal deformation of sediments associated with this process is little known and is the main topic of investigation in this report.

### LOCATION AND GEOLOGIC SETTING

The study area is located off the northern Alaska coast between 150°00" and 152°00" west long. and 70°30" and 71°00" north lat. in the Beaufort Sea off the Colville River delta in Harrison Bay (Figure 1a and b). Water depths in the study area range from approximately two meters near the Colville delta, to 20 meters in the northern part.

The coastline in the study area is being eroded at the rate of approximately 2.5 m/yr, except for the eastern, active part of the Colville Delta, which is accreting (Reimnitz et al., in press). This erosion creates coastal bluffs that are typically 2 to 3 m high but may reach a height of 6 meters (Reimnitz and Barnes, 1974; Reimnitz et al., in press). The line of bluffs is broken by the impingement of several river systems whose general morphological character consists of low prograding deltaic mudflats at the river mouths (Reimnitz and Barnes, 1974). The coastal plain is an area of low broad relief capped by tundra vegetation. This coastal plain is underlain by Tertiary to Pleistocene and Holocene moraines, glaciomarine deposits, erratic-bearing gravel, eolian sand, gravel, sand and silt (Black, 1964; Payne et al., 1951; Carter, 1983b).

The continental shelf in the area is generally flat and remains shallow for a considerable distance from shore (Reimnitz and Barnes, 1974). A detailed examination of shelf topography shows it to be extremely rough on a small scale. The small scale morphological character of the shelf is dominated by the presence of long linear criss-crossing grooves produced by the grounding of ice keels below pressure ridges (Barnes et al., 1984). The grooves are characterized by troughs and ridges that are typically 1 m deep and 7 m wide (Barnes et al., 1984), although some may reach 10 m deep and 30 m wide (Barnes and Rearic, 1985) (Figure 2).

The surface sediments on the shelf are dominantly

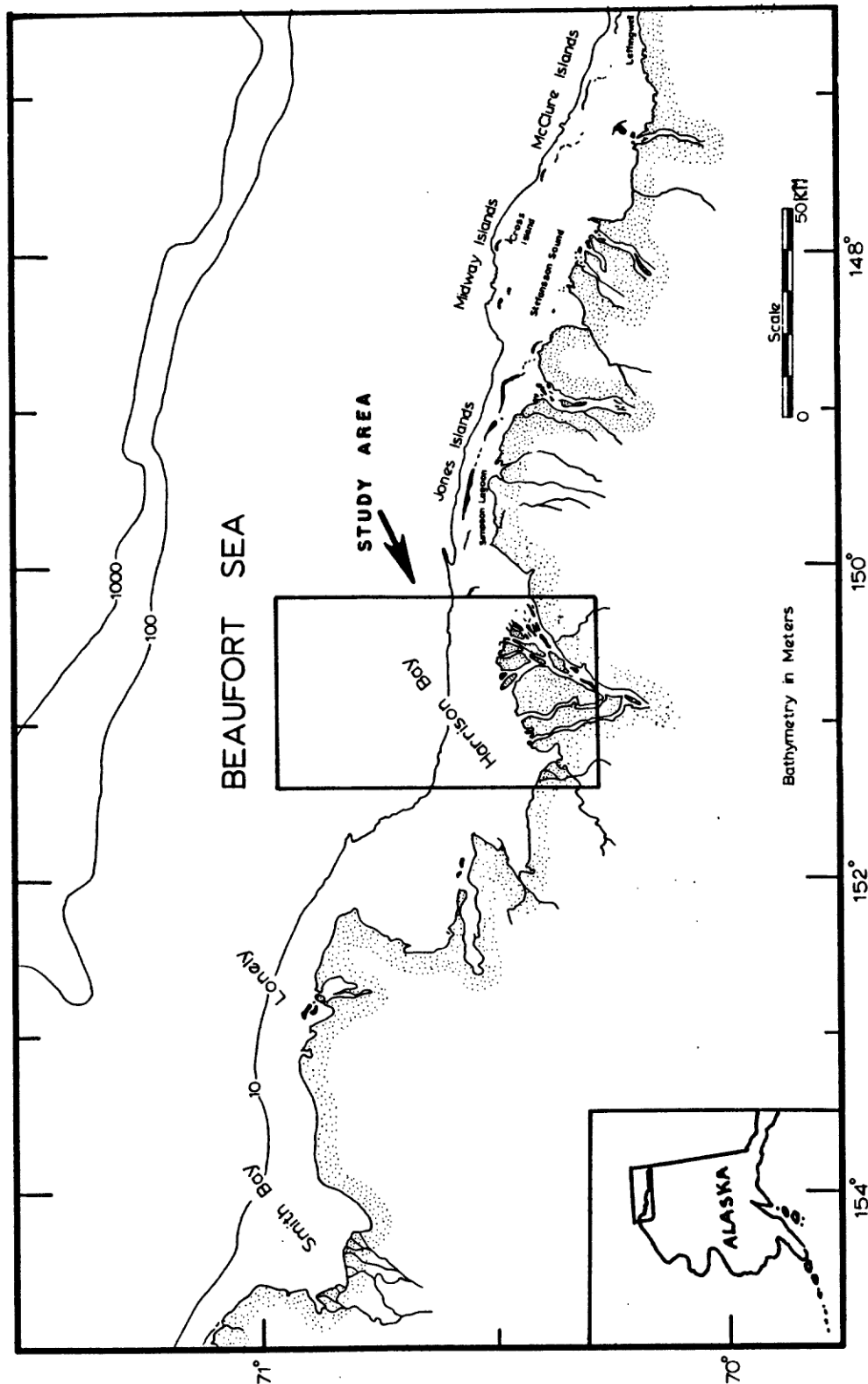


Figure 1a. Locality map showing position of study area in relation to the north Alaskan coast.

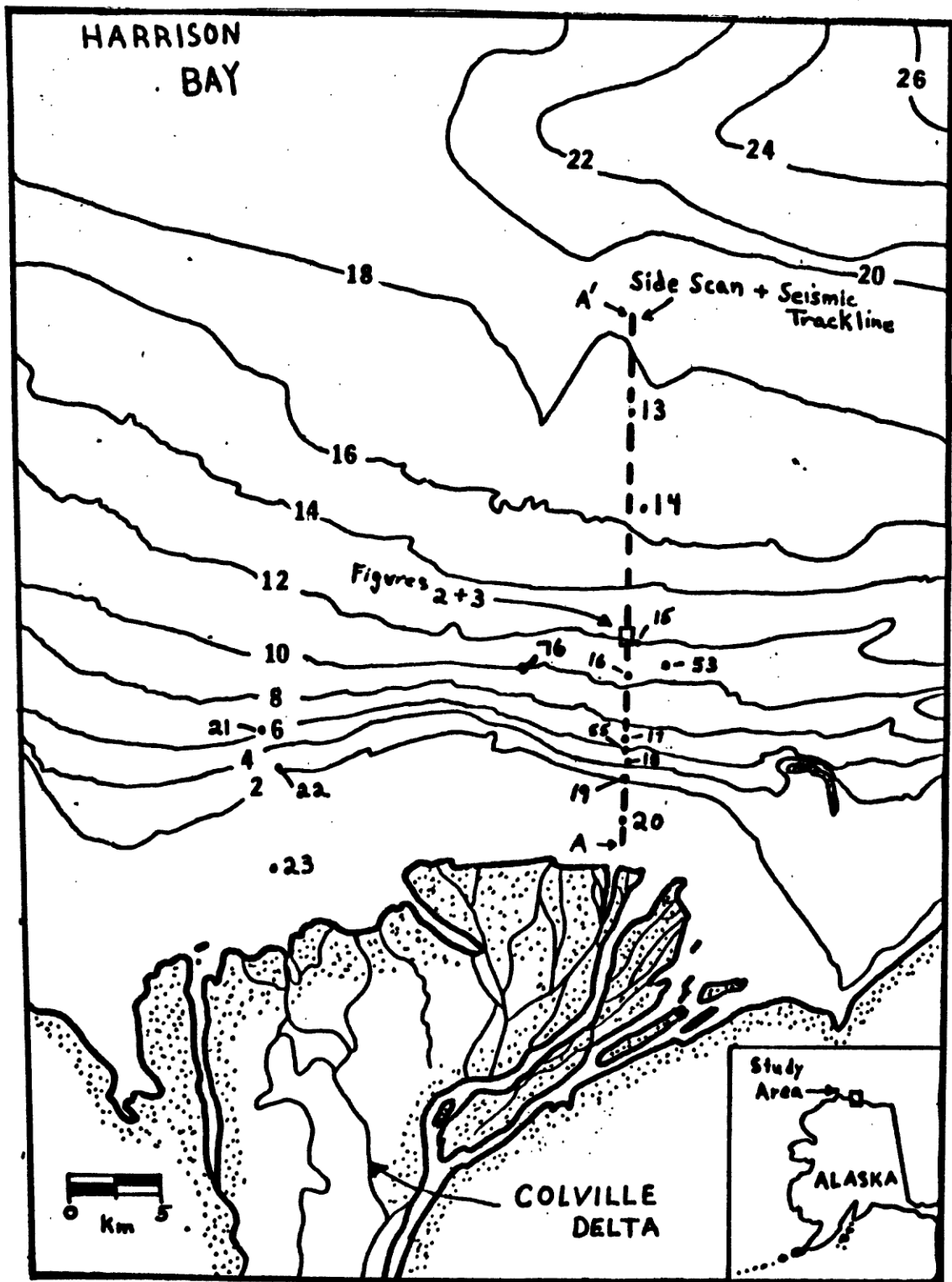
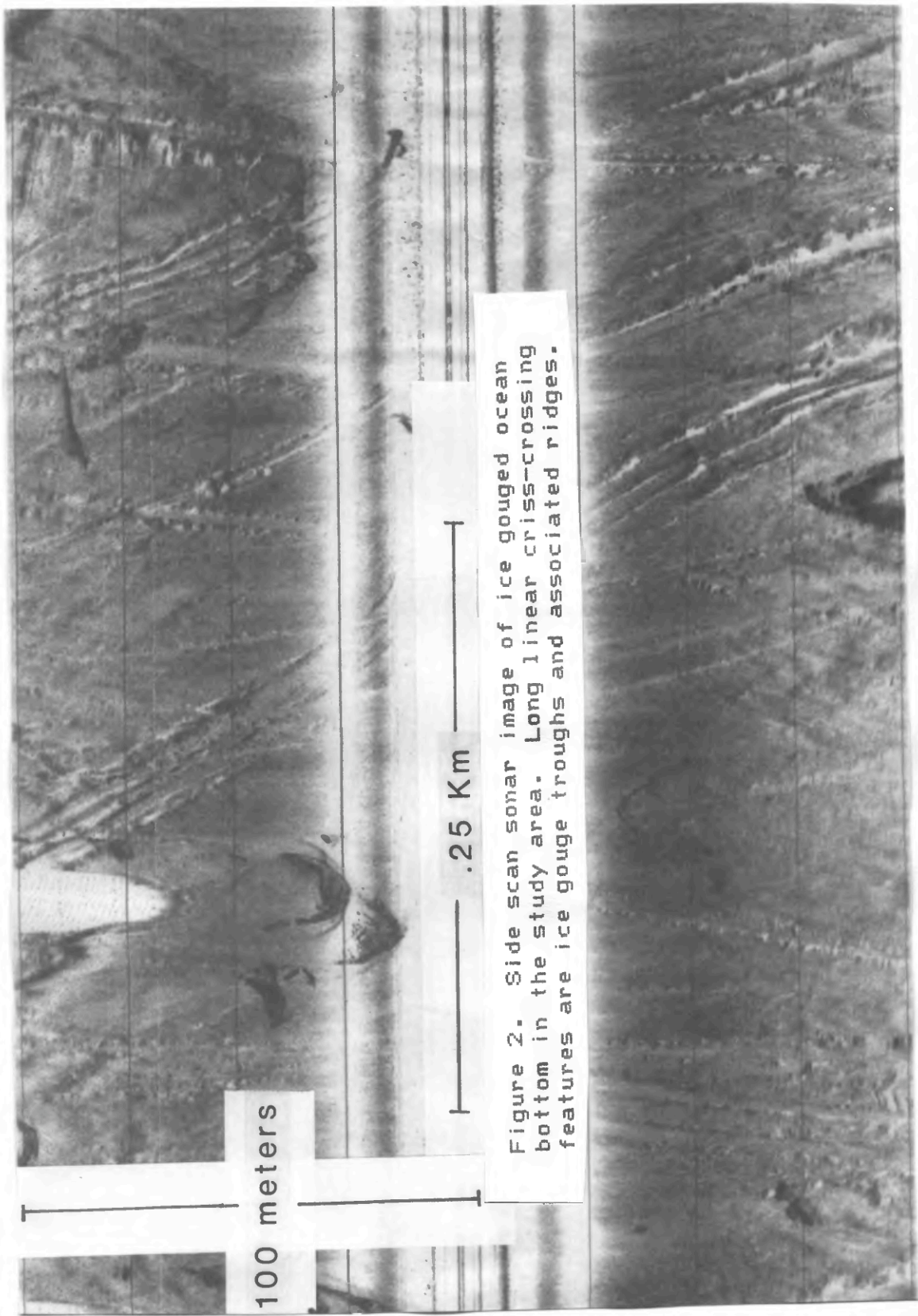


Figure 1b. Detailed locality map of Harrison Bay showing bathymetry (2 m interval), core localities, ships track line, and location of side scan image and seismic profile in figure 2 and 3. Vessel track line is labeled A-A' and corresponds to shelf profile in figure 19.



100 meters

.25 Km

Figure 2. Side scan sonar image of ice gouged ocean bottom in the study area. Long linear criss-crossing features are ice gouge troughs and associated ridges.

fine mud, clay and sand, but gravel and occasional boulders are encountered (Barnes and Reimnitz, 1974). The Colville River and eroding coastal bluffs are introducing large amounts of fibrous organic matter to the sea, and some is found incorporated in recent sediments (Barnes et al., 1979).

#### PREVIOUS WORK

One of the earliest investigations on the process of ice gouging was done by Tarr (1897) who observed and documented the effects of grounded ice on sediments. Emery (1949) and Carsola (1954) performed early studies of the topography and sediments in the Beaufort Sea, while Rex (1955) described sea-floor microrelief caused by grounded sea ice in the northern Chukchi Sea. More recent work defining characteristics and rates of ice gouging was done by Kovacs (1972), Pelletier and Shearer (1972), Barnes and Reimnitz (1972, 1973, 1974), Reimnitz and Barnes (1972, 1973, 1974), Barnes et al. (1973, 1979, 1985), Reimnitz et al. (1972, 1973, 1974), and Kempema (1983) analyzed the stratigraphy of an individual ice gouge. Naidu (1974), and Naidu et al. (1971, 1972, 1974) analyzed clay mineralogy, sedimentation, and sediment geochemistry of the Beaufort Sea. Yorath et al. (1970) interpreted seismic profiles and sediments of the Beaufort Sea.

#### PURPOSE OF INVESTIGATION

The major emphasis of this report is to:

- 1) Ascertain what sedimentary structures, textures, and lithologies characterize deposition in an arctic shelf environment that is influenced by a large fluvial system.
- 2) Delineate the type of deformational structures that may be overprinted on the sediments in that environment through ice-sediment interaction.
- 3) Describe in detail cores collected in the Harrison Bay area of the Beaufort Sea during 1976 and 1977 by the United States Geological Survey branch of Pacific Marine Geology.

The study area was chosen because the north-south transect of available cores might provide a cross-section through surficial sediments on the shelf perpendicular to the coastline, from a shallow deltaic environment to the midshelf at 20 m, where ice gouging may strongly influence deposition.

#### METHOD OF STUDY

The cores were gathered using a vibratory coring device lowered from the research vessel to the sea floor. A pair of electrically driven, counter rotating, eccentric weights in the core head rapidly hammers

against an anvil driving the core barrel into the sediment (Barnes et al., 1979). After retrieval, cores were capped with paraffin or plaster of Paris to seal them and were subsequently shipped to Menlo Park, California for laboratory processing (Barnes et al., 1979).

Cores obtained during the 1976-1977 field seasons were sliced longitudinally and resin peels and x-ray radiographs were made from each core. A visual examination of cores, peels and radiographs has been undertaken in this study, as outlined below.

#### CORE EXAMINATION PROCEDURE

Each of the 15 available cores were examined together with their corresponding peels and radiographs. Each radiograph had a corresponding black and white contact print made from it for ease in description. The contact prints were attached to boards and lithologic as well as structural information obtained from the cores and peels was written directly onto the margin of each appropriate board. In this way, the prints could then be laid out together with all the corresponding information. The prints were then overlain with clear acetate, and all sedimentary structures were traced in detail to better ascertain their type and possible origin. This method provided a wealth of information and proved best for this study.

### GENERAL GEOLOGY

#### THE COASTAL PLAIN

The subaerial coastal plain in the vicinity of Harrison Bay and the Colville River consists of a broad plain of low relief mantled by Quaternary and Recent sediments that rest unconformably on Mesozoic sedimentary rocks (Walker, 1976). This area received minimal glaciation during Quaternary time (approximately 10%) (Walker, 1976; Dinter, 1982). The glacial and glaciofluvial deposits which resulted contribute to the sediment load of the Colville River and its tributaries at present (Walker, 1976).

The sediments that mantle the coastal plain consist of late Cenozoic marine, lacustrine, alluvial, glacial, and eolian deposits (Carter, 1983b), referred to as the Gubik Formation (Carter, 1986) and the glaciomarine deposits are known as the Flaxman Formation (Carter, 1986).

The most prominent geologic structure in the area is the Barrow Arch, a buried ridge of Early Paleozoic rocks deformed during the Ellesmerian orogeny. The

structure is overlain by Late Paleozoic and Mesozoic rocks that arch over the crest of the ridge, and are truncated by an unconformity. The unconformity is capped by Cretaceous shale (Stearn et al., 1979).

The coastal plain in the study area is geomorphically dominated by the presence of the Colville River Delta. The Colville River has created a delta that has an areal exposure of approximately 600 sq. km. The delta is approximately 40 km from its apex to the ocean, and is approximately 45 km wide along its front (Walker, 1973). The Colville River is the largest river in arctic Alaska, and has a drainage basin dimension of 60,000 sq. km (Walker, 1976).

#### THE SHELF

The continental shelf off the north coast of Alaska was subaerially exposed to approximately the 100m isobath as a result of a eustatic sea level minimum, caused by late Wisconsin glaciation (Dinter, 1982; Dillon and Oldale, 1978). The glacial maximum and sealevel minimum occurred approximately 17,000 years ago (Dinter, 1982; Dillon and Oldale, 1978). The shelf at that time formed an unconformable surface which has been delineated seismically and assigned a tentative age of Pleistocene, based on the timing of the retreat of the last glaciation (Craig and Thrasher, 1982; Dinter, 1982). In the study area, Holocene sediments that overlie the unconformity are believed to reach a thickness of no greater than 5m (Reimnitz and Barnes, 1974).

The Quaternary sediments have been delineated seismically into three generalized units by Craig and Thrasher (1982). The surficial Holocene unit is 0 to approximately 5 m thick and consists of an acoustically transparent layer displaying vague, continuous bedding subparallel to the seafloor. The underlying Holocene-Pleistocene boundary consists of a strong continuous reflector cut locally by shallow channels and low terraces (Figure 3a and b). The Pleistocene unit has been broken into two units (A and B respectively) based on acoustic character, only unit A can be recognized in the study area.

The upper boundary of unit A consists seismically of a diffuse to sharp reflecting surface that is commonly characterized by a very jagged or "jumpy" appearance (Figure 3a and b). The surface of unit A is believed to correlate in appearance to the morphological features of the present day coastal plain, including V-shaped stream channels, thaw lakes, beach ridges, and thermokarst topography (Craig and Thrasher, 1982).

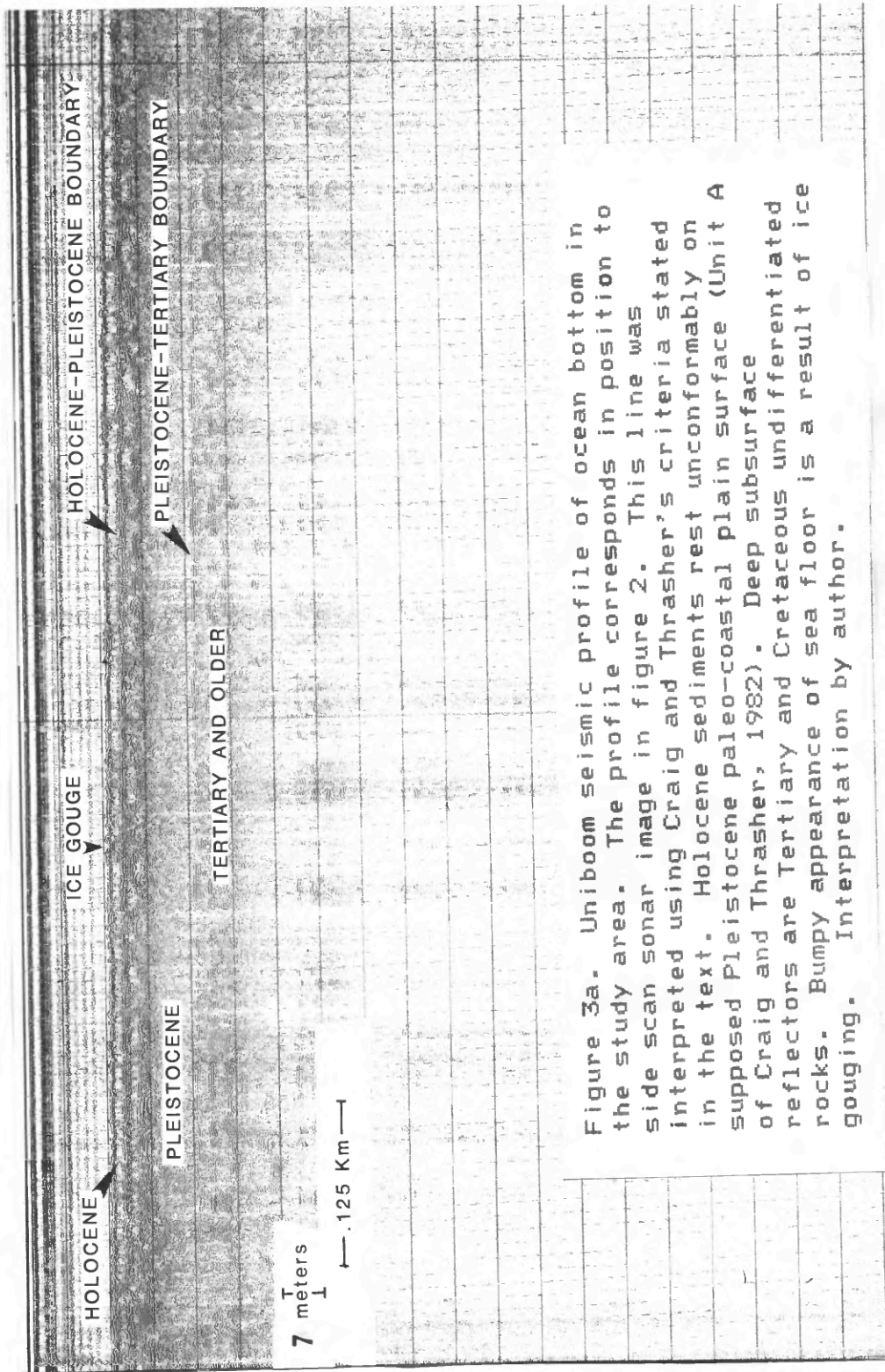


Figure 3a. Uniboom seismic profile of ocean bottom in the study area. The profile corresponds in position to side scan sonar image in figure 2. This line was interpreted using Craig and Thrasher's criteria stated in the text. Holocene sediments rest unconformably on supposed Pleistocene paleo-coastal plain surface (Unit A of Craig and Thrasher, 1982). Deep subsurface reflectors are Tertiary and Cretaceous undifferentiated rocks. Bumpy appearance of sea floor is a result of ice gouging. Interpretation by author.

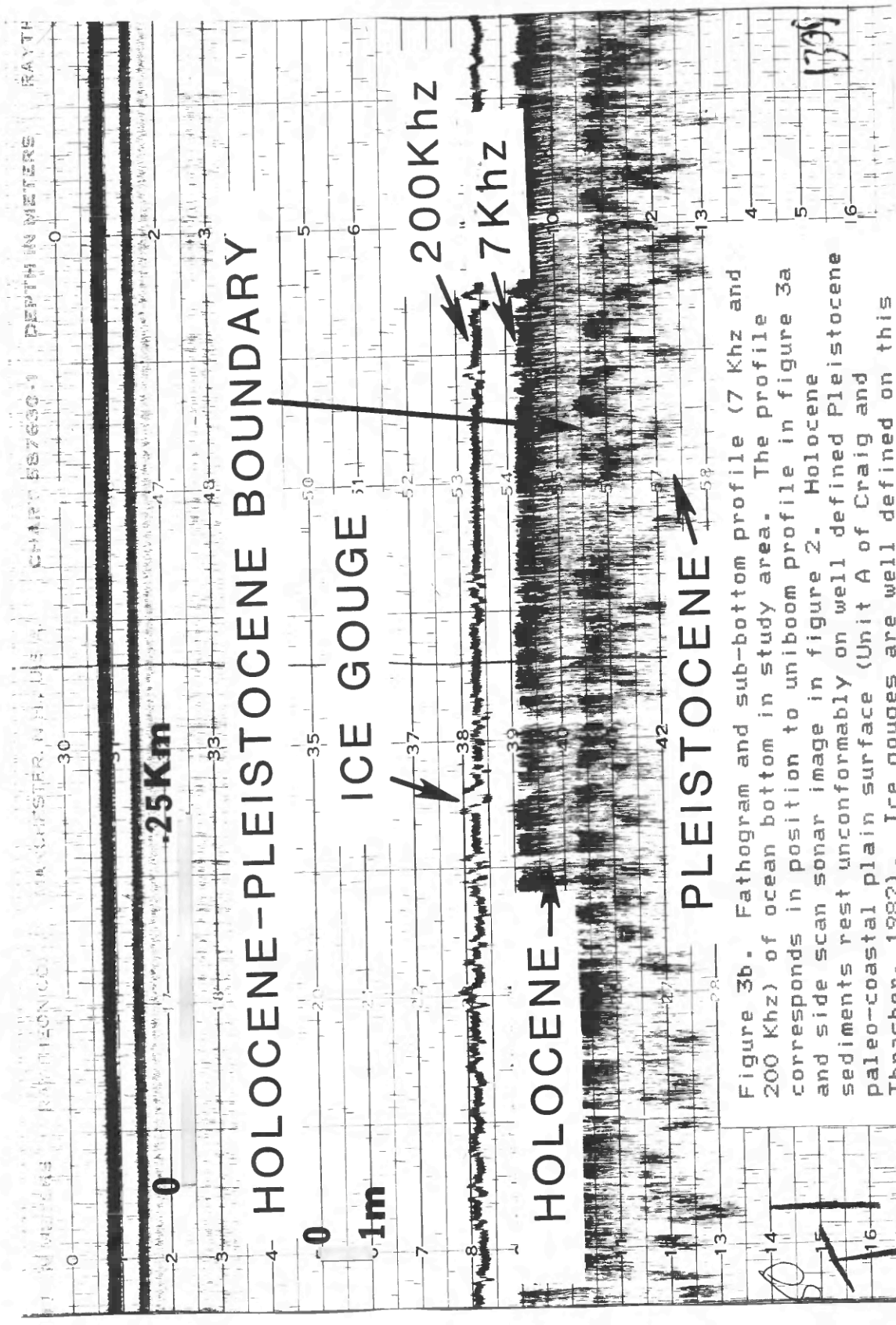


Figure 3b. Fathogram and sub-bottom profile (7 KHz and 200 KHz) of ocean bottom in study area. The profile corresponds in position to uniboom profile in figure 3a and side scan sonar image in figure 2. Holocene sediments rest unconformably on well defined Pleistocene paleo-coastal plain surface (Unit A of Craig and Thrasher, 1982). Ice gouges are well defined on this profile at seafloor as very jagged peaks and troughs. Interpretation by author.

Unit B seismically consists of a sharp, strongly reflective surface of uniformly low relief that is believed to represent a marine deposit contemporaneous with unit A. Several morphological features indicative of a marine environment such as sedimentary bedforms, beaches, and offshore bars have been interpreted (Craig and Thrasher, 1982). The contact between unit A and unit B represents a facies change and generally follows the 20m isobath. The almost vertical contact is very abrupt and is interpreted as a shoreline bluff several meters high. The morphological expression of the shoreline is not reflected at the seafloor (Craig and Thrasher, 1982). It should be noted that the inferred shoreline corresponds in position to the inner edge of the stamukhi zone of Reimnitz et al. (1978), an area of intense ice reworking by pressure-ridge keels. Unit A and unit B are approximately 10 to 12 m thick in the study area (Barnes, 1987, personal communication), and are believed to correspond to the Gubic Formation onshore (Craig and Thrasher, 1982).

Units A and B unconformably overlie Late Cretaceous and Tertiary undifferentiated sedimentary rocks known as "Colville Group and younger rocks" and consist of shale and laterally discontinuous sand bodies characteristic of a regressive marine sequence (Craig and Thrasher, 1982).

#### GENERAL CORE DESCRIPTIONS AND ENVIRONMENTS OF DEPOSITION

In this section, each core is first described and then assigned a depositional environment based on lithologic, textural, and structural criteria. Photographs of peels and radiographs are used to illustrate and support each case. Detailed descriptions of individual cores can be found in Appendix A.

The cores studied in this report display characteristics of several distinct depositional environments when compared to sediments described by Tucker (1981), Reineck and Singh (1980), and Reading (1986) from lower latitude shelves. The depositional environments are on occasion overprinted by deformation caused by ice-sediment interaction and by coring.

The general sedimentological characteristics described for a lower offshore depositional environment are laminated to highly bioturbated muds, derived from suspension settling, interbedded with parallel laminated, occasionally ripple laminated, fine grained sands, derived from storm-generated currents (Tucker, 1981; Reineck and Singh, 1980; Reading, 1986). This environment is usually found in water depths greater than 10 m (Tucker, 1981; Reineck and Singh, 1980;

Reading, 1986).

Reineck and Singh (1980) and Reading (1986) describe an upper offshore environment in water depths of 2 to 10 m as consisting of muddy fine sand, interbedded with parallel laminated and bioturbated mud and sand.

Tucker (1981), Reineck and Singh (1980), and Reading (1986) describe distal prodelta deposits as consisting of laminated, fine grained muddy sediments, dominantly clay and silty clay, that can be transitional into either upper offshore or lower offshore shelf deposits. Prodelta sediments proximal to the delta front environment are slightly more coarse grained and display a variety of bedforms including ripple bedding, small scale graded bedding, and lenticular laminations (Reineck and Singh, 1980).

Tucker (1981), Reineck and Singh (1980), and Reading (1986) describe delta front deposits as consisting of parallel laminated sand and silt, interbedded with parallel laminated and occasionally ripple laminated silty and sandy clays and organic detritus.

Deformational features found in the cores were classified to either of two origins: coring-related deformation, or ice-related deformation. Coring-related deformation encompass all structures that display a consistent concave-down nature, that is, laminations or bedding whose ends at the edge of the core were distinctly bent down as a result of penetration of the core barrel. Also any highly deformed sediments at the bottom of a core were suspect, and were believed to have been derived from suction created at the bottom of the core when it was extracted from the bottom.

Ice-related deformational features vary greatly, but in general consist of laminations or bedding that display a consistent concave up nature, or any highly deformed area (ie. folded or offset) that is bounded on top and bottom by horizontally laminated or bedded sediments.

#### HARRISON BAY SAMPLES

##### CORE V-13

Core V-13 was extracted from 19 m of water, approximately 37 km from shore. Normal neritic deposition is represented by massive to laminated, bioturbated clay and silty clay deposits (Figure 4b, arrow 1) (Tucker, 1981; Reading, 1986). Interbedded, horizontally laminated, fine grained silty sands probably represent intermittent coarser grained deposition by storm currents (Figure 4b, arrow 2) (Tucker, 1981; Reading, 1986). Deformation in the lower

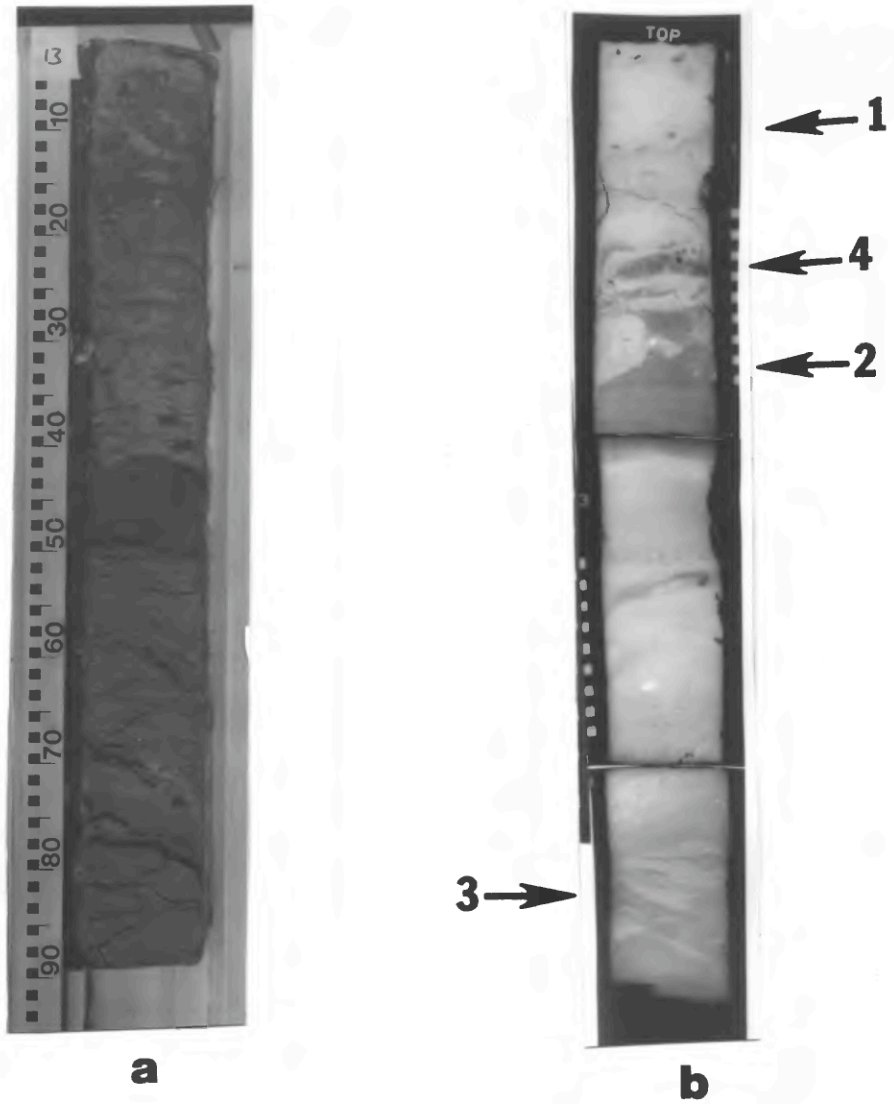


Figure 4a and b. A and b are peel and radiograph photographs respectively of core V-13. Arrow 1 points to clay, arrow 2 points to sand. Arrow 3 points to coring artifact in lower portion of core. Arrow 4 points to loaded contacts. Scale is in cm.

part of this core is an artifact produced by coring (Figure 4b, arrow 3). The massive to laminated clay and silty clay, interbedded with thin units of fine grained silty sand are characteristics for deposition in a lower offshore shelf environment (Tucker, 1981; Reineck and Singh, 1980; Reading, 1986).

#### CORE V-14

Core V-14 was extracted from 15 m of water, approximately 29 km from shore. Normal neritic shelf deposition is represented by massive to slightly laminated, clay and silty clay (Tucker, 1981; Reading, 1986). Bedded fine sand, pebbles, and shell fragments in upper part of core probably represent deposition from storm currents (Figure 5a and b, arrow 1) (Tucker, 1981; Reading, 1986). Deformation is a result of coring. The massive to laminated clay and silty clay, interbedded with thin units of fine sand containing pebbles and shell fragments may be indicative of deposition in a lower offshore shelf environment (Tucker, 1981; Reineck and Singh, 1980; Reading, 1986).

#### CORE V-15

Core V-15 was extracted from 12.4 m of water, approximately 20 km from shore. Normal neritic sedimentation is represented by sandy and silty clays (Reading, 1986). The presence of coarse material (sand and silt) incorporated with the clay is possibly indicative of higher terrigenous input resulting from closer proximity to shore, or wave winnowing resulting from closer proximity to wave base. Horizontally laminated, fine to very fine grained sands and silty sands may represent deposition from storm currents and normal bottom currents (Tucker, 1981). Tabular crossbedding is present in middle part of core and is probably the result of sandwave propagation (Reineck and Singh, 1980) (Figure 6a and b). This core is physically deformed in its lower part. Rip up clasts (Figure 6b, arrow 1) are believed to be the result of ice gouging, and highly contorted bedding (Figure 6b, arrow 2) are believed to be the result of coring. The sandy and silty clays may be indicative of deposition in a lower offshore shelf environment, or an upper offshore shelf environment, and is probably a transitional zone between the two (Tucker, 1981; Reineck and Singh, 1980; Reading, 1986).

#### CORE V-16

Core V-16 was extracted from 11.5 m of water, approximately 16 km from shore. This core is composed of highly deformed clay, sandy clay, and sand (Figure 7a and b). Physical mixing of the sediment in this area

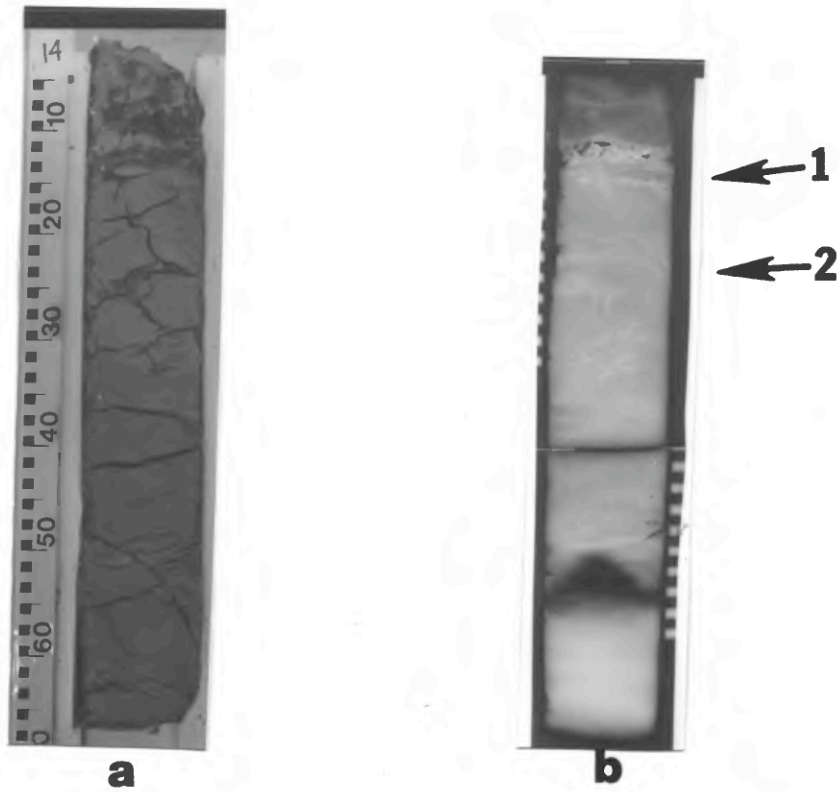
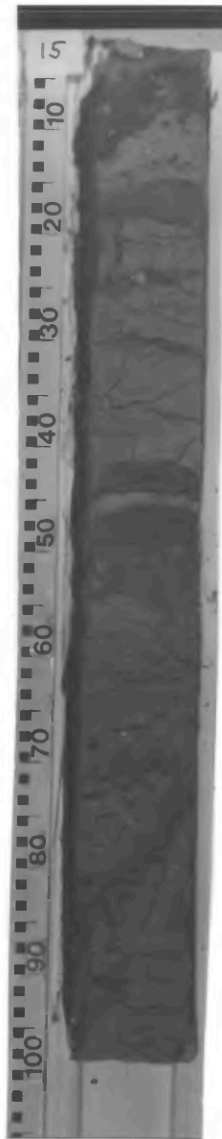


Figure 5a and b. A and b are peel and radiograph of core V-14. Arrow 1 points to bedded fine sand, pebbles, and shell fragments in upper portion of core. Arrow 2 points to concave down laminations. Scale is in cm.



**a**



**b**

Figure 6a and b. A and b are peel and radiograph of core V-15. Arrow 1 points to rip-up clasts, arrow 2 points to deformed bedding. Arrow 3 points to loaded contacts. Scale is in cm.

due to ice gouging has obliterated the common structural and textural criteria normally used to classify sediments to an environment of deposition. Also the possible influence of prodelta muds from the Colville river delta may have delivered a high percentage of clay to this depositional environment. Original horizontal laminations have been deformed into highly contorted bedding in the upper part of the core (Figure 7b, arrow 1), and have been physically folded and offset in the lower part of the core (Figure 7b, arrow 2), probably by ice keel turbation. This core probably represents deposition in the upper offshore shelf environment, and has been classified based upon the position of the core in the transect relative to other cores in the study, and the water depth from which it was extracted, rather than by the sedimentological evidence.

#### CORE V-17

Core V-17 was extracted from 8.5 m of water, approximately 10 km from shore. This core is composed of highly deformed clay and silty clay (Figure 8a and b). The normal sequence of horizontally laminated clays has been overprinted by the effects of ice gouging and most of the sediments in the core are deformed (Figure 8b, arrow 1). Some of the deformation in this core is likely the result of the coring procedure itself, however, only the concave down laminations (Figure 8b, arrow 2) may be directly assigned to this category. The overall fine grained character of the sediments in this core relative to the water depth from which it was extracted and its proximity to the Colville River delta is indicative of a prodelta depositional environment (Reineck and Singh, 1980; Reading, 1986).

#### CORE V-18

Core V-18 was extracted from 3.3 m of water, approximately 9 km from shore. The upper portion of this core consists of horizontally laminated clay, sandy clay, and sand interbeds with high organic content (Figure 9a and b). Cross-laminated and ripple cross-laminated sands are abundant in this portion of the core as well as thin beds (2 cm or less) of organic detritus. Truncation of horizontal and cross-laminations is present resulting in small cut and fill structures. The thin horizontally laminated clay and cross laminated sand interbeds and high organic content in this portion of the core may be indicative of the delta front depositional environment (Figure 9b, arrow 1) (Tucker, 1981; Reineck and Singh, 1980; Reading, 1986).

The lower portion of this core is composed of

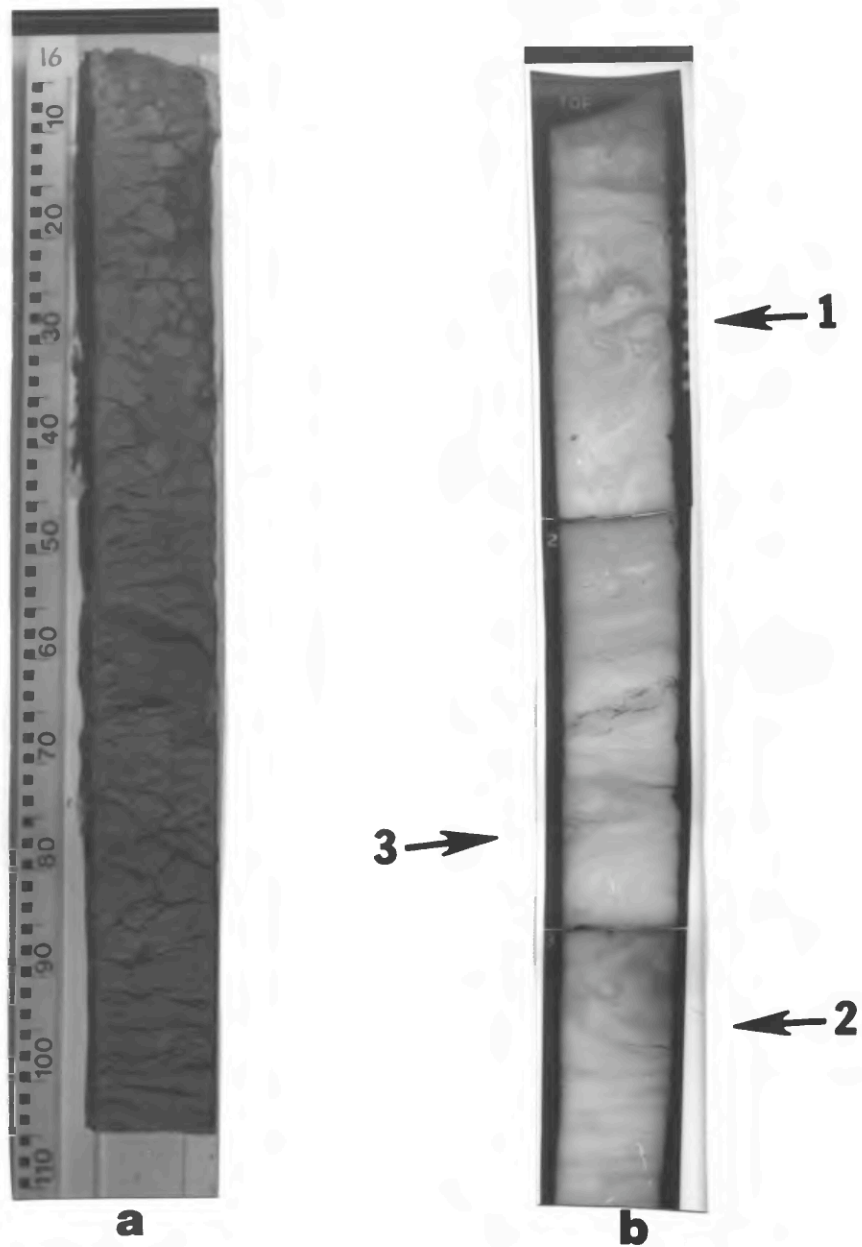
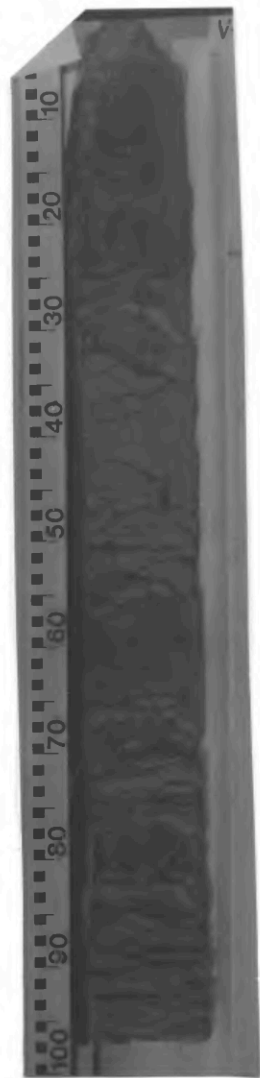


Figure 7a and b. A and b are peel and radiograph of core V-16. Arrow 1 points to highly deformed bedding in upper portion of core. Arrow 2 points to folded and faulted bedding in lower portion of core. Arrow 3 points to small rip-up clast incorporated in folded beds. Scale is in cm.



**a**



**b**

Figure 8a and b. A and b are peel and radiograph of core V-17. Arrow 1 points to probable ice gouge related deformation. Arrow 2 points to coring derived deformation. Arrow 3 points to rip up clasts. Scale is in cm.

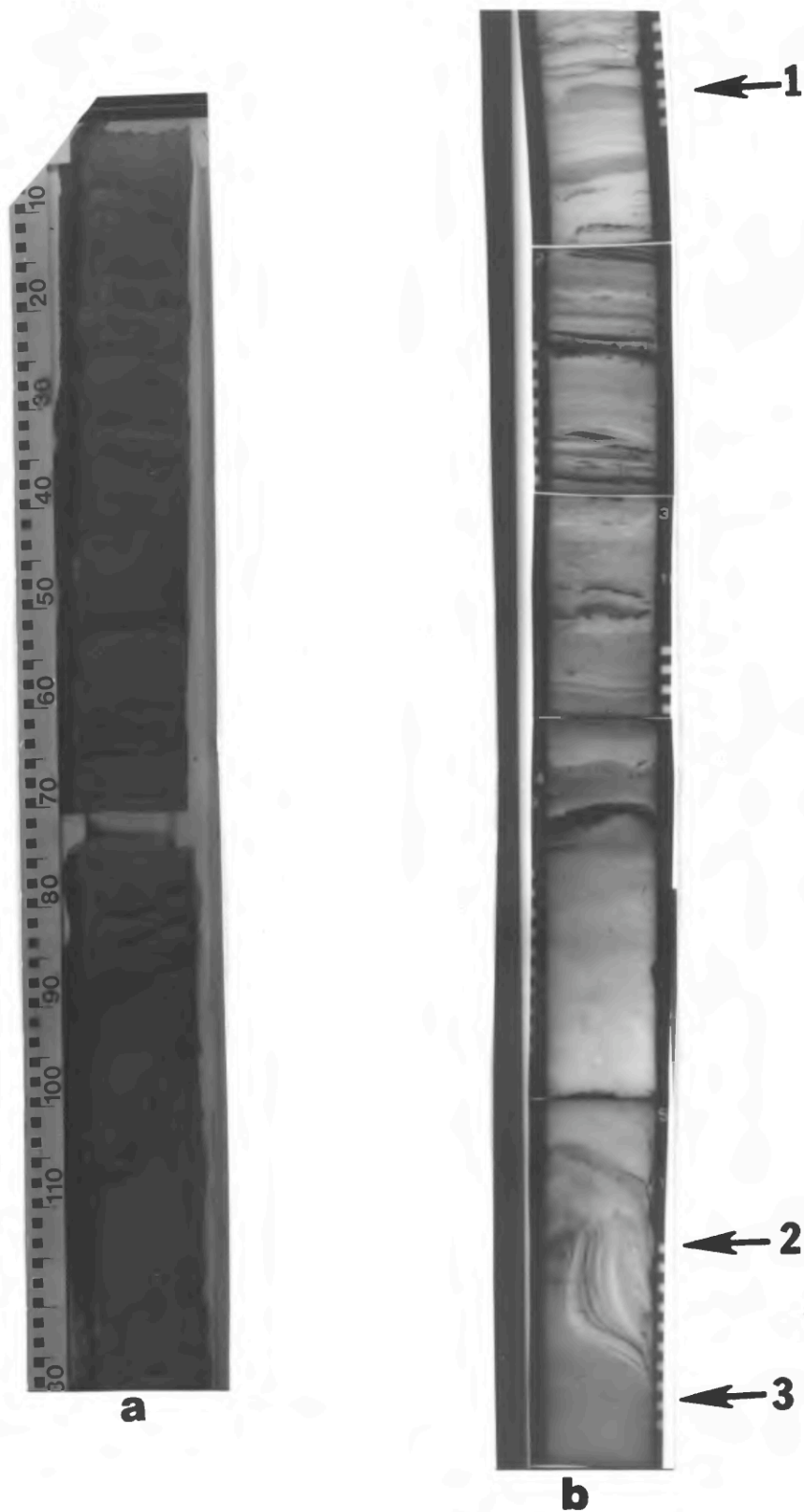


Figure 9a and b. A and b are peel and radiograph of core V-18. Arrow 1 points to horizontally laminated sands, silts, and clays of the delta front. Arrow 2 points to highly deformed bedding that may be a result of ice gouging. Arrow 3 points to clay with abundant rootlets that may represent a subaerially exposed marsh deposit. Scale is in cm.

massive clay and sandy clay beds with few sand and organic interbeds. The lower 50 cm of the core shows extreme deformation of a sandy unit above a massive clay unit with abundant rootlets and plant stems (Figure 9b, arrow 2). The presence of the rootlets may indicate that this portion of the core was a mat of tundra vegetation that has subsequently been buried. However, because this part of the core is dominantly mud (approximately 85%), and a tundra mat would most likely contain a larger organic component (ie. >15% organics), this interpretation is improbable. The presence of rootlets in mud may indicate subaerial exposure (Reineck and Singh, 1980; Reading, 1986), and this portion of the core therefore may represent deposition in a tidal marsh environment (Figure 9b, arrow 3) (Reineck and Singh, 1980; Reading, 1986; Tucker, 1981).

#### CORE V-19

Core V-19 was not physically available for study in this project, but prior description of this core by Barnes and Reimnitz, and its position in the sampling transect warrants the discussion of the depositional environment for this sample.

Core V-19 was extracted from the delta front in 2 m of water, approximately 7 km from shore. The core consists of horizontally laminated, medium to fine grained sand, clayey sand, clay, and organic interbeds (Figure 10a and b). Some bioturbation is seen in the upper portion of the core, and ripple cross-lamination is present in the middle portion of the core (Figure 10b, arrow 2). A high percentage of coal concentrates is present in the sands as thin laminae and as component grains. The horizontally laminated sand, clay, and organic interbeds may be indicative of deposition in the delta front environment (Figure 10b, arrow 3) (Tucker, 1981; Reineck and Singh, 1980; Reading, 1986).

#### CORE V-20

Core V-20 was extracted from the delta front in 1.5 m of water, approximately 3 km from shore. The core consists of horizontally laminated sand, sandy clay, clay, and organic interbeds (Figure 11a and b). Areas of mottling and possible bioturbation are present. The horizontally laminated sand, clay and organic interbeds may be indicative of deposition in the delta front environment (Figure 11b, arrow 1) (Tucker, 1981; Reineck and Singh, 1980; Reading, 1986). A 25 cm long U-shaped fold is present in the upper half of the core (Figure 11b, arrow 2), as well as a truncated overturned fold in the lower half (Figure 11b, arrow 3). These structures are believed to be the result of ice-keel turbation.

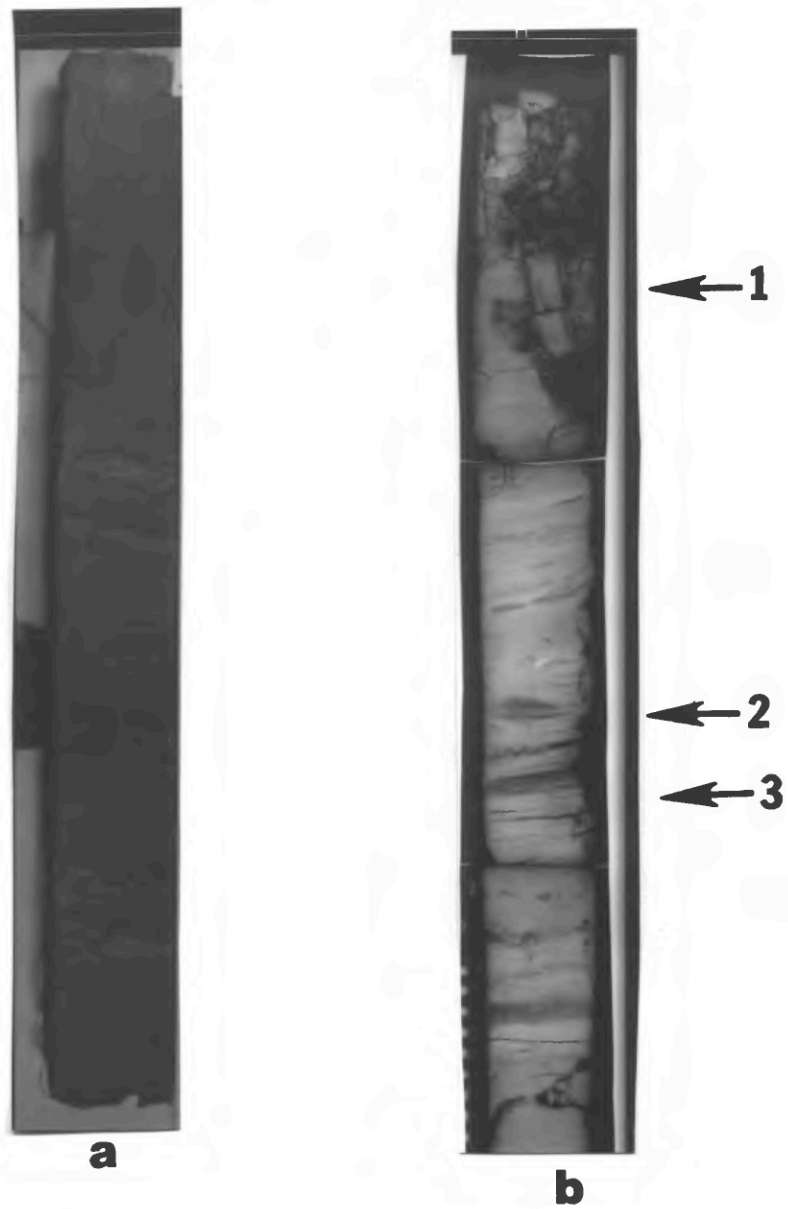


Figure 10 a and b. A and b are peel and radiograph of core V-19. Arrow 1 points to large burrow in upper portion of core. Arrow 2 points to cross laminations. Arrow 3 points to horizontally laminated sands and silts of the delta front. Scale is in cm.

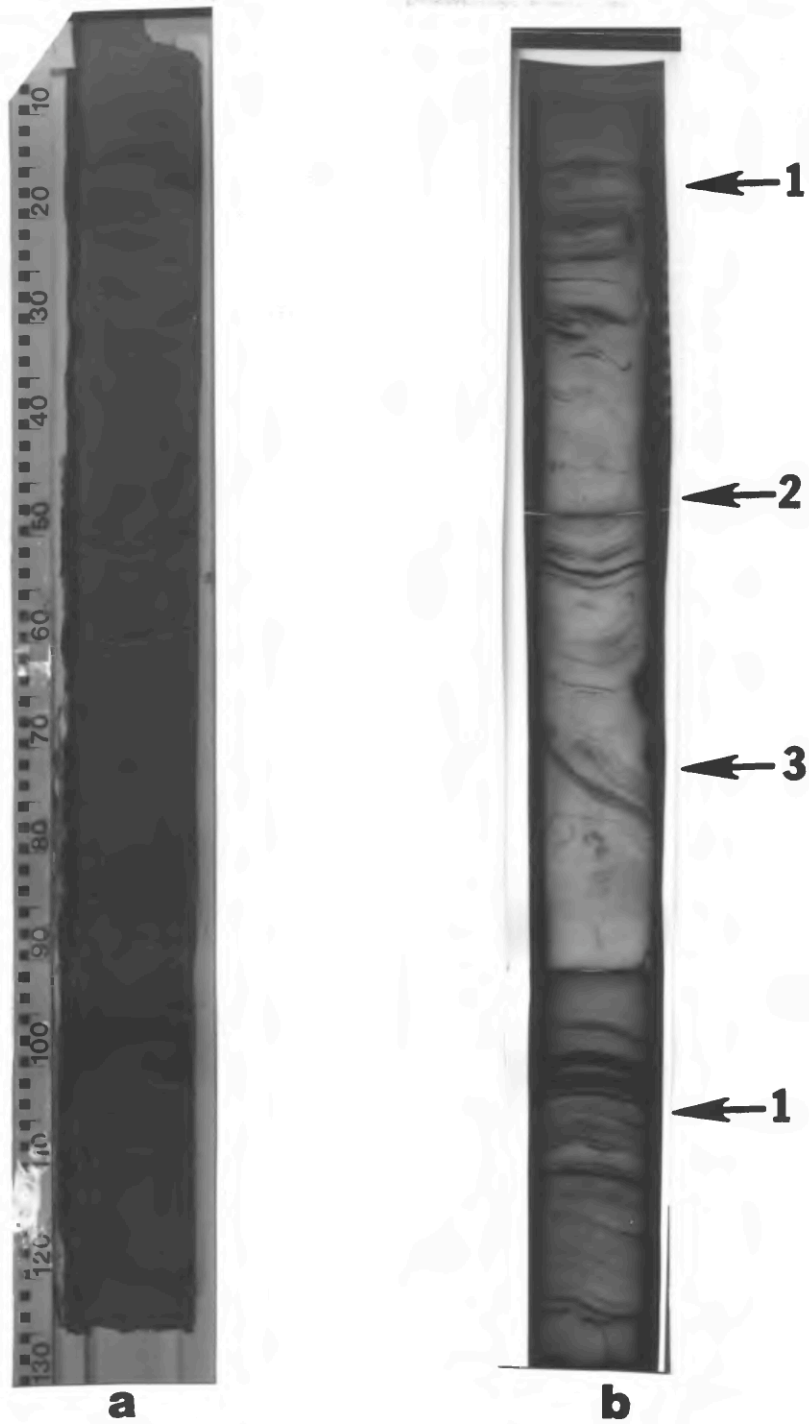


Figure 11a and b. A and b are peel and radiograph of core V-20. Arrow 1 points to undeformed horizontally laminated sediments of the delta front. Arrow 2 points to large box fold in upper portion of core. Arrow 3 points to truncated overturned fold in lower portion of core. Scale is in cm.

#### CORE V-21

Core V-21 was extracted from 4 m of water, approximately 18 km from shore. The core consists of horizontally laminated sand, clay, and organic interbeds commonly indicative of the delta front depositional environment (Figure 12a and b) (Tucker, 1981; Reineck and Singh, 1980; Reading, 1986). Clay units in the upper portion of the core are extensively bioturbated and mottled (Figure 12b, arrow 1). Wavy and contorted contacts indicative of ice overloading are dominant (Figure 12b, arrow 2). The upper 25 cm of the core displays highly contorted and deformed bedding (Figure 12b, arrow 3), and these structures are believed to have resulted from ice gouging.

#### CORE V-22

Core V-22 was extracted from .6 m of water, approximately 15 km from shore. The upper portion of this core consists of horizontal to steeply dipping laminated and cross laminated sands. The sands are relatively clean, but contain visible fibrous organic matter. At 50 cm a large bedform consisting of planar crossbeds and ripple cross laminations exist. A minor portion of this structure consists of well bedded, cross and planar laminated peat. This portion of the core represents a shoaling upward of sediments and is indicative of deposition in a subaqueous distributary mouth bar (Figure 13b, arrow 1) (Reineck and Singh, 1980; Reading, 1986). The lower portion of this core consists of horizontally laminated, partially deformed, sand, clay, and organic interbeds which may suggest deposition in the delta front depositional environment (Figure 13b, arrow 2) (Tucker, 1981; Reineck and Singh, 1980; Reading, 1986). Some bioturbation is evident in this portion of the core, and organic content is highly visible.

#### CORE V-23

Core V-23 was extracted from the delta front in 1 m of water, approximately 6 km from shore. The core consists of horizontally laminated and ripple cross-laminated sand, clay, and organic interbeds (Figure 14b, arrows). Some climbing ripple cross laminations are evident. Abraded twigs and plant stems are abundant in the upper portion of the lower half of the core. Bioturbation and mottling are restricted to a few small units. No deformation is seen in the core, although some wavy contacts that may be indicative of ice-overloading do exist (Figure 14a and b). The horizontal and ripple cross laminated sand, clay and organic interbeds may be indicative of deposition in the

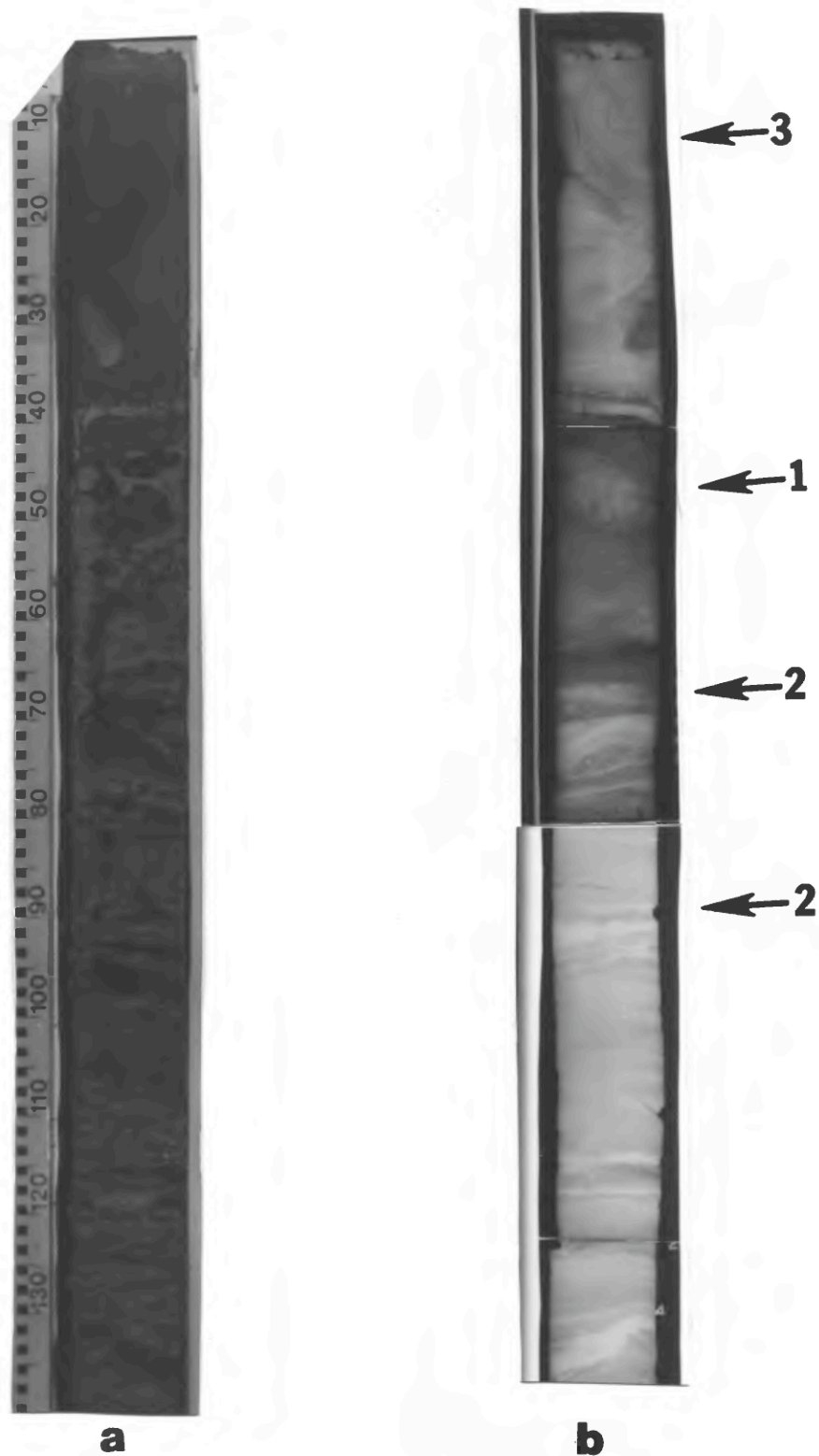


Figure 12a and b. A and b are peel and radiograph of core V-21. Arrow 1 points to bioturbated horizon. Arrow 2 points to wavy and undulatory contacts. Arrow 3 points to highly deformed bedding in upper portion of core. Scale is in cm.

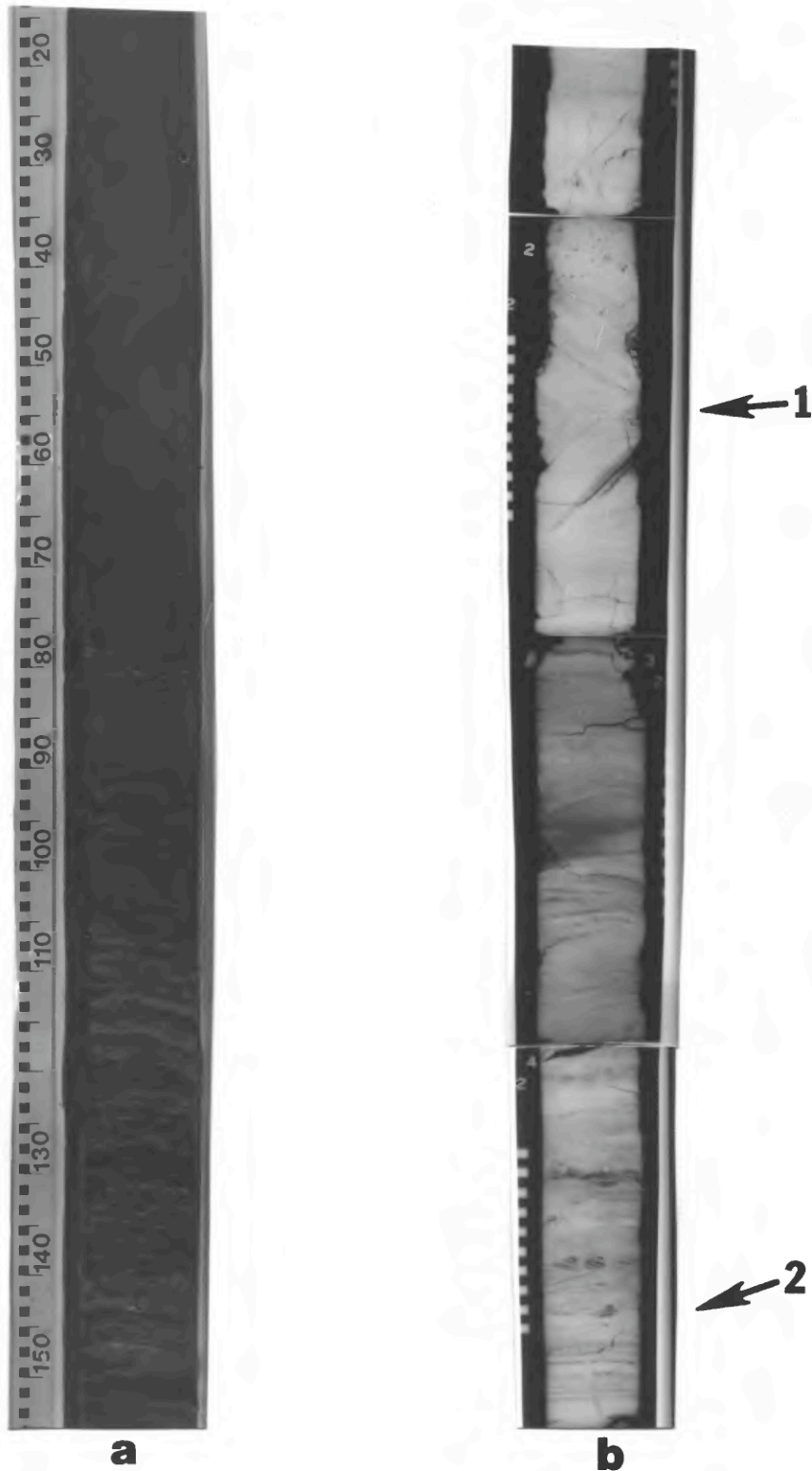
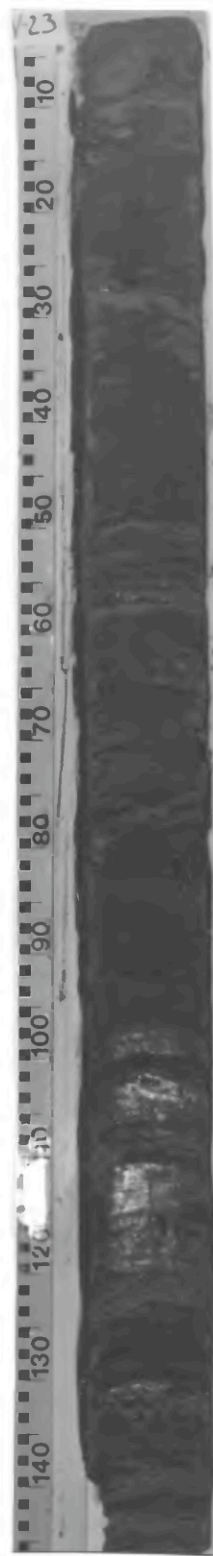
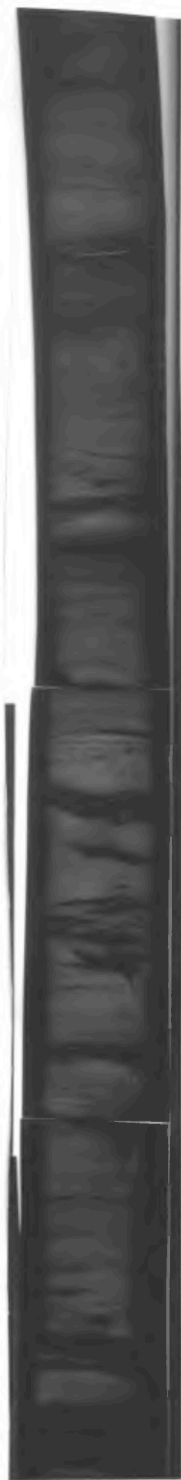


Figure 13a and b. A and b are peel and radiograph of core V-22. Arrow 1 points to steeply dipping laminated and cross laminated sands of the distributary mouth bar. Arrow 2 points to horizontally laminated sediments of the delta front. Scale is in cm.



**a**



**b**

Figure 14a and b. A and b are peel and radiograph of core V-23. Arrow points to dark areas which represent organic interbeds. Scale is in cm.

delta front environment (Tucker, 1981; Reineck and Singh, 1980; Reading, 1986).

#### CORE V-53

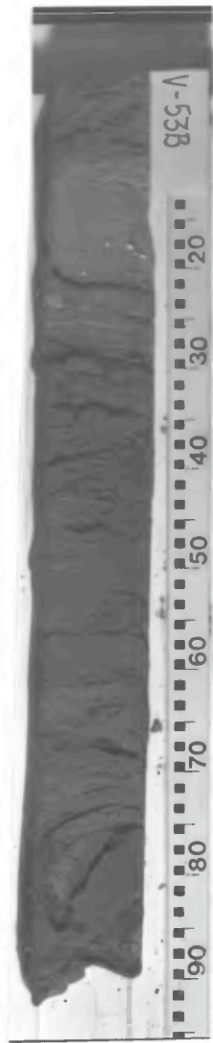
Core V-53 was extracted from 13 m of water, approximately 20 km from shore. The core consists of horizontally laminated sand, sandy clay, and clay interbeds. The sands are clean, lensoidal and cross laminated in part, and may be the result of storm currents and current reworking and suggest deposition in the upper offshore environment (Reineck and Singh, 1980; Reading, 1986). The horizontally laminated clay units represent normal neritic deposition from suspension settling, which is believed to have been influenced by the high influx of suspended sediment from the prodelta region (Reineck and Singh, 1980; Reading, 1986) (Figure 15a and b). The bottom portion of this core is slightly deformed, most likely from coring (Figure 15b, arrow 1).

#### CORE V-55

Core V-55 was extracted from 7 m of water, approximately 10 km from shore. The upper half of this core consists dominantly of massive to partially laminated clay, interbedded with thin sand units (Figure 16a and b, arrow 1) that may be indicative of deposition in the prodelta environment (Tucker, 1981; Reineck and Singh, 1980; Reading, 1986). The clay is believed to have been deposited from suspension by sediment-laden water of the river (Reineck and Singh, 1980; Reading, 1986), and by current and ice reworking (Reimnitz and Barnes, 1974; Barnes et al., 1979). The sand units may be derived from storm-generated currents, or strong current reworking (Reineck and Singh, 1980; Reading, 1986). The lower half of this core consists of thin, horizontally laminated sand, sandy clay, and clay units that may be indicative of the delta front environment (Figure 16b, arrow 2) (Tucker, 1981; Reineck and Singh, 1980; Reading, 1986). Minor cross bedding and wavy contacts are present, organic material is notably absent. The middle portion of this core shows a high degree of deformation that is bounded on top and bottom by horizontally laminated sediments, most likely the result of ice gouging (Figure 16b, arrow 3).

#### CORE V-76

Core V-76 was extracted from 10.7 m of water, approximately 12 km from shore. This core was reported by Barnes and Reimnitz (1977) to have been taken on top of a sediment wave, (which were typically less than 1 m high) a hydraulically produced mega-ripple bedform. The upper 1/3 of the core consists of finely laminated,



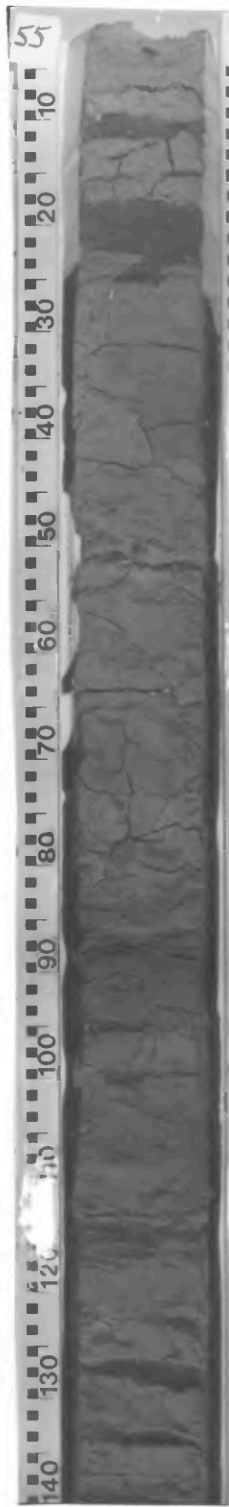
**a**



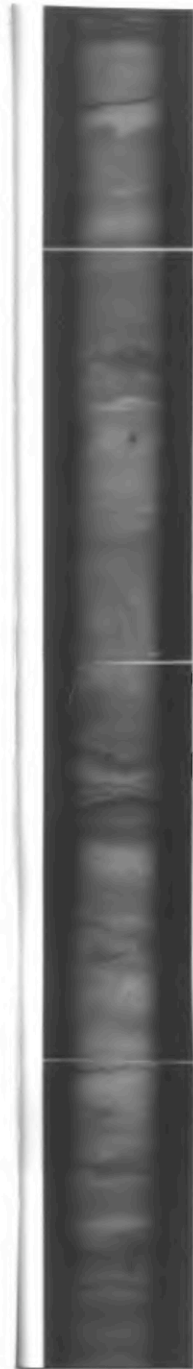
**b**



Figure 15 a and b. A and b are peel and radiograph of core V-53. Arrow 1 points to coring artifact in lower portion of core. Scale is in cm.



**a**



← 1

← 3

← 2

**b**

Figure 16a and b. A and b are peel and radiograph of core V-55. Arrow 1 points to massive to partially laminated sediments of the prodelta, and loaded deformed contact. Arrow 2 points to horizontally laminated sediments of the delta front. Arrow 3 points to probable ice deformation. Scale is in cm.

medium to coarse-grained clean sand with minor silt interbeds. These sediments probably represent deposition in the sediment wave that was sampled (Figure 17, arrow 1). A prominent scour and fill structure is present in the middle of this portion and all laminations are pronouncedly deformed into a concave-up fold structure, deformation is probably the result of ice gouging (Figure 17, arrow 2).

The lower 2/3 of this core consists of highly bioturbated and mottled clay and finely laminated sand interbeds suggesting deposition in the delta front environment (Figure 17, arrow 3) (Tucker, 1981; Reineck and Singh, 1980; Reading, 1986). The clay contains abundant shell fragments and whole shells and displays no bedding. The sand is horizontally and trough cross-laminated, medium to fine grained, and clean. Some rip-up clasts of clay with high organic content are present.

## DISCUSSION

### DEPOSITIONAL ENVIRONMENTS

The analysis of cores in this study was undertaken with two major questions in mind: 1) What sedimentary structures, textures, and lithologies characterize deposition in an arctic shelf environment that is encroached upon by a major fluvial system; and 2) What type of deformational structures may be overprinted on the sediments in this environment through ice-keel turbation?

It was assumed that the sedimentological character of each core reflected its depositional environment when sampled. This assumption appears to be well founded based on the sedimentological evidence present in the cores. This assumption fails in the event that the sea floor in the study area is erosional, in which case the depositional environments described may reflect Early Holocene deposition rather than present processes. In all cases, the sedimentological characteristics of each core were compared to the sedimentological characteristics of similar environments (i.e., water depth, distance from shore, sediment influx) on lower latitude shelves that have been well documented in the literature (Tucker, 1981; Reineck and Singh, 1980; Reading, 1986). In any instances where sedimentary features in the cores diverged from documented features of the particular depositional environment in question, and no other source of information could be found that described such a feature, it was assumed that such a feature is peculiar to deposition in that environment on high latitude shelves. The following discussion is a summary of general sedimentological features displayed

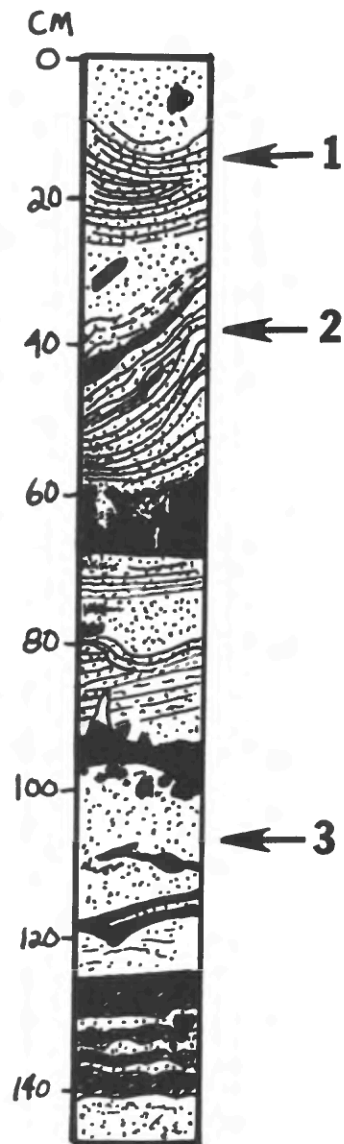


Figure 17. Sketch of core V-76. Peel and radiograph photographs not available for this core. Arrow 1 points to sediment wave deposit. Arrow 2 points to highly deformed laminations. Arrow 3 points to delta front deposits. Scale is in centimeters.

in the offshore to onshore transect through the study area.

The water depths, depositional environments, and stratigraphy of cores V-13, V-14, and V-15 compared well to the lower offshore shelf environment. Sediments described from low latitude, lower offshore shelf environment in depths of 10 to 30 m, generally consist of muds, laminated to highly bioturbated, derived from suspension settling, interbedded with parallel laminated, occasionally ripple laminated, fine grained sands, derived from storm generated currents (Tucker, 1981; Reineck and Singh, 1980; Reading, 1986). Cores V-13 and V-14 consist of massive to faintly laminated clays interbedded with horizontally laminated fine grained sands (Figures 4 and 5). Core V-15 displayed characteristics of both lower and upper offshore shelf environments (Figure 6). The upper offshore shelf is characterized by muddy fine sand admixed and interbedded with the sediments (mud and sand) of the lower offshore shelf (Reineck and Singh, 1980; Reading, 1986).

Determining the depositional environment for core V-16, 4 km inshore of core V-15 (Figure 1b) was complicated by the overprinted deformation associated with ice gouging. The assignation of this core to the upper offshore shelf environment relies more on general lithologic trend relative to position with other cores in the transect, actual position of core V-16 in the transect, and the water depth (11.5 m) from which it was extracted. Core V-16 has a higher percentage (visual estimate) of sand than does core V-15. In the classical shelf environment, where ice does not play a dominant role, the upper offshore shelf zone proximal to the lower shoreface (Reineck and Singh, 1980) would contain thicker and more abundant sand interbeds than the distal upper offshore shelf (Reineck and Singh, 1980; Reading, 1986). In core V-16 the higher percentage of sand that might normally be associated with proximal upper offshore shelf is present, but clay appears to be dominant in the lithology. It is this author's belief that the apparent abundance of clay is due to the proximity of the Colville Delta and the influence of prodelta muds in the area. The sand present is not in the form of interbeds, but rather as an admixture with clays, believed to result from vigorous reworking by ice and currents. Barnes et al., (1979) hypothesized that bedding would not survive in an area of vigorous seabed scouring by grounded ice keels. Perhaps the distinct units of sand and clay seen in core V-13 and V-14 are reworked by ice gouging into the highly deformed sandy clay seen in core V-16 (Figure 7).

Core V-53 is spatially located in the transect

between, and to the east of, V-15 and V-16. While the core is from a similar setting as cores V-15 and V-16, it does not display the same characteristics of vigorous ice reworking shown in V-15 and V-16. Only the lower portion of the core displays distinct deformation and is composed of sandy clay (Figure 15b, arrow 1). Cores V-16 and V-53 are believed to represent a transitional zone between upper offshore shelf deposition and prodelta deposition.

Cores V-17 through V-23, and V-55 were all extracted onshore of the 10 m isobath and show a trend from offshore to onshore of increasing degrees of fluvially dominated sedimentation. Cores V-17 and V-55 show a relative shoreward increase in clay content and a decrease in fine sand content (visual estimation) (Figure 8 and 16) and represent the prodelta environment.

All of the cores taken landward of the 2 m isobath are conspicuously similar. Sedimentation at the 2 m isobath is a dramatic change from massive clays offshore to thin finely laminated clay and fine sand interbeds shoreward. It is this author's opinion that the 2 m isobath represents the approximate seaward limit of the delta front. Cores V-18 through V-23 all represent deposition on the delta front.

Cores V-17 through V-23, and V-55 were compared to the delta front and prodelta environments described by Tucker (1981), Reineck and Singh (1980), and Reading (1986). Figure 18a and b shows cores taken from the Guadalupe Delta (from Reineck and Singh, 1980), displaying the characteristics of natural levee, marsh, delta front, and prodelta environments. Cores from the Colville Delta (Figures 8, 9, 10, 11, 12, 13, 14, and 16) show a striking similarity with those of the Guadalupe Delta. The most marked similarity is that of the cores of the delta front and prodelta. The natural levee, and marsh environments were not cored in this study, and therefore no comparison can be made.

The sediments from the Colville Delta are generally more fine grained, but the overall similarity in the morphological character between the sets of cores is impressive.

In summary, the cores from Harrison Bay generally display a trend from offshore to onshore, of muds deposited from suspension settling, interbedded with fine sands derived from storm currents on the lower offshore shelf at depths greater than 10 m (Figure 19), to increasingly more sandy sediments to about the 10m isobath (upper offshore shelf). In the vicinity of the 10 m isobath a transition zone between upper offshore shelf and prodelta environments is present, characterized by the muds of the prodelta admixed and

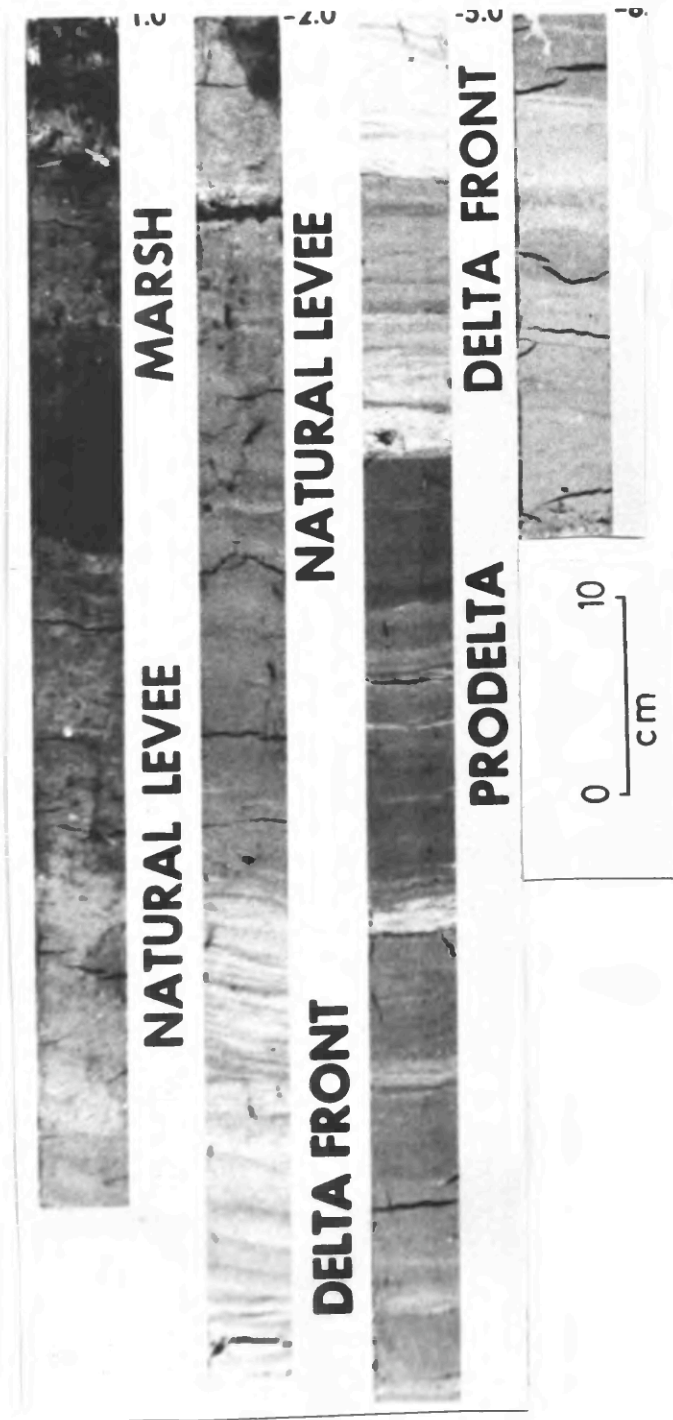


Figure 18a. Cores from the Guadalupe Delta showing characteristics of delta front, prodelta, and marsh deposits. Compare the characteristics of these cores with cores from the study area (From Reineck and Singh, 1980).

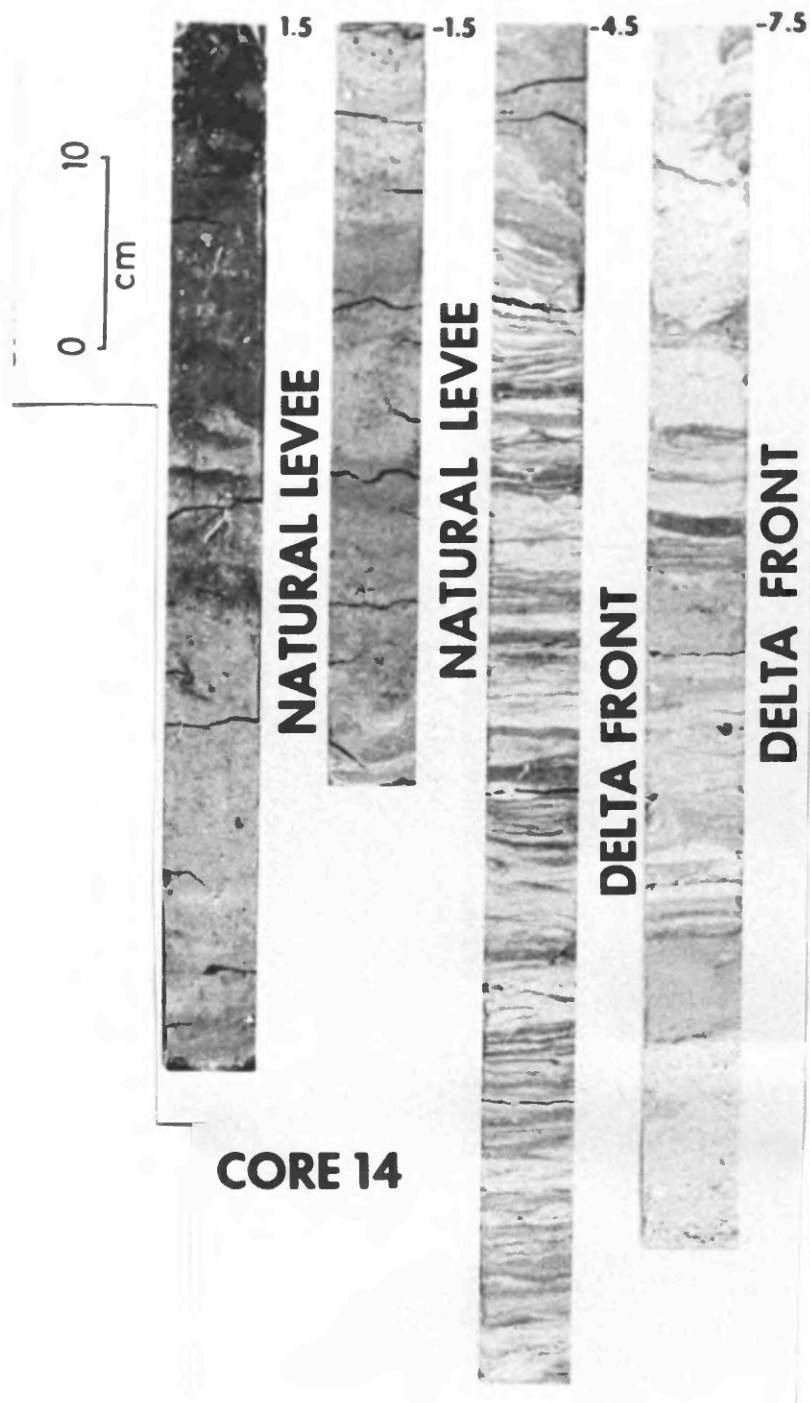


Figure 18b. More cores from the Guadalupe Delta. Compare these cores with cores from the study area (From Reineck and Singh, 1980).

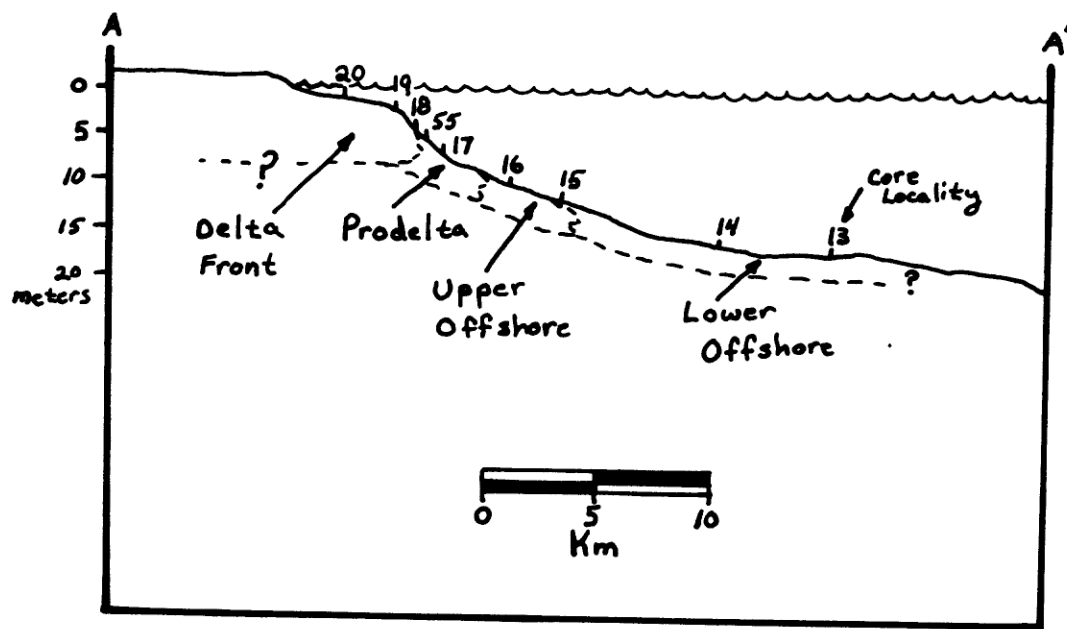


Figure 19. Shelf profile along ship's trackline and coring transect (A-A') showing core localities and hypothetical facies associations.

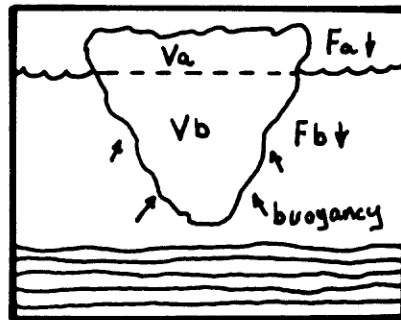
interbedded with the muddy fine sand of the upper offshore. Shoreward of the 10 m isobath to approximately the 2 m isobath is the prodelta environment characterized by partially laminated very fine grained sediments (Figure 19), and shoreward of the 2 m isobath is the delta front environment that is characterized by thin horizontally laminated interbeds of clay, sand, and organic detritus (Figure 19).

#### ICE-RELATED DEFORMATION

The literature on ice keel deformation of the seabed is sparse (Reimnitz and Barnes, 1974; Barnes et al., 1979; Reineck and Singh, 1980). Models discussing the formation of ice gouges are abundant (see previous work section), however no models discussing seabed deformation associated with ice gouging have been found. The following hypothesis is proposed for ice-related deformation.

The process of ice gouging, regardless of genetic form (that is either pack-ice related or ice-berg related) leaves evidence in the stratigraphic record in the form of either the preserved gouge or the deformation associated with the process of gouging. As an ice keel plows through the seabed, it leaves in its wake a groove cut into the soft sediments of the ocean floor. As the ice keel passes through the sediment, two forces are acting simultaneously upon it. The horizontal force acting as the transport mechanism (i.e., wind, currents, rotation of the ice pack, etc.), and the vertical force based on the weight of the ice supported by the seabed due to gravity. In Figure 20a,  $V_a$  represents the volume of ice above the waterline when the ice is completely buoyant (equilibrium), and  $V_b$  represents the volume of ice below the waterline at equilibrium. The mass of the ice above the waterline when the ice is not moving can then be represented by  $F_a$  where  $F_a = (V_a \times \text{density of sea ice}) \times \text{gravity}$ , and the mass of the ice below the waterline can be represented by  $F_b$  where  $F_b = (V_b \times \text{density of seawater} - \text{density of sea ice}) \times \text{gravity}$ . The net force exerted downward ( $F_{net}$ ) then will be equal to  $F_{net} = F_a - F_b$ .  $F_{net} = 0$  when the buoyancy forces acting on the ice below the waterline balance with force exerted by the mass of the ice above the waterline. Because of the density difference between ice and water the ice floats with approximately 1/5th of its volume above the waterline (Kovacs and Mellor, 1974; Gross, 1982).

In the case where ice is touching the bottom (Figure 20b),  $V_a$  becomes  $V_a + \text{some newly exposed volume } (V_{new})$  above the water after touching the bottom, here called  $V_1$ . The force then acting above the waterline ( $F_a$ ) becomes  $F_a = ((V_a + V_{new}) \times \text{density of sea ice} \times$

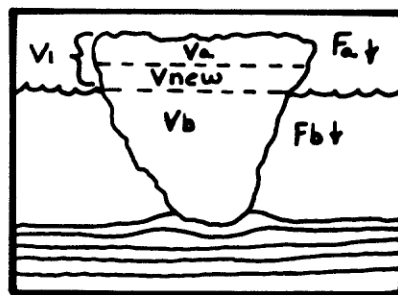


$$F_a = (V_a \cdot \rho_{ice}) \cdot g$$

$$F_b = (V_b \cdot \rho_{H_2O} - \rho_{ice}) \cdot g$$

$$F_{net} = F_a - F_b = 0$$

a

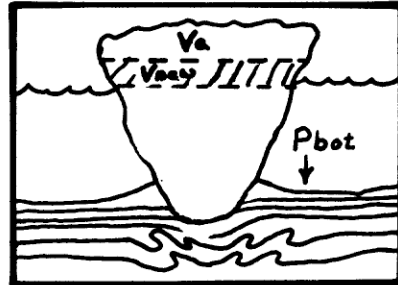


$$F_a = V_1 \cdot \rho_{ice} \cdot g$$

$$F_b = (V_b - V_{new}) \cdot (\rho_{H_2O} \cdot \rho_{ice}) \cdot g$$

$$F_{net} > 0$$

b



$$P_{bot} = \frac{F_{net}}{\text{Surface Area of Keel touching bottom}}$$

c

Figure 20a through 20c. Graphic representation of hypothetical model of ice gouging. A) Floating ice,  $F_a$  equals  $F_b$  so net force = 0. B) Ice touching bottom, new total volume exposed above waterline is  $V_1$  ( $V_a + V_{new}$ ),  $F_a$  is not equal to  $F_b$  and the net force,  $F_{net}$ , is greater than 0 by the amount of mass in  $V_{new}$ . C)  $P_{bot}$  is pressure exerted on bottom by ice keel. This model can be likened to a woman standing in high heels, large weight distributed over small surface area creates great pressures.

gravity), and the force acting below the waterline is  $F_b = (V_b - V_{new}) \times [(\text{density of seawater}) - (\text{density of sea ice})] \times (\text{gravity})$ . The net force acting on the bottom in this case is  $F_{net} = F_a - F_b$  where  $F_{net}$  will be  $>0$  by the amount of mass in  $V_{new}$ .

If we now consider the net force acting on the bottom and the disequilibrium between the size of the ice mass relative to the size of the ice keel contacting the bottom we can see that the forces acting on the bottom from a grounded ice keel can be tremendous. To look at this example in terms of pressure, let's call the pressure exerted on the bottom as  $P_{bot}$ .  $P_{bot}$  then becomes  $P_{bot} = F_{net} / \text{surface area of the ice keel touching bottom}$ .

A typical cross-sectional dimension of a pressure ridge is roughly 35 m wide at the waterline and the width of the keel is roughly 5 m at the bottom (Kovacs and Mellor, 1974). These proportions can be likened to a woman wearing high heeled shoes. The large mass of the woman distributed over the very small surface area of the bottom of the high heel creates extremely large pressures. In the case of the ice keel, the large mass of ice above the waterline distributed over the small surface area of the keel touching the bottom creates great pressures. In this case, the pressures exerted on the bottom by such a geometry are great, certainly enough to deform soft sediments.

There are obviously other factors that play a role in the deformation of any substrate, but this discussion is only a basic explanation and the inclusion of other factors here is beyond the scope of this report. For a more in-depth analysis of the physics and ice forces refer to Kovacs and Mellor (1974).

In all cases, except where ice just touches bottom, some type of subsurface deformation probably occurs in soft sediments. The combination of loading by the weight of the ice, coupled with a horizontal translation, caused by transport processes, plows the seabed at the surface, and may result in lateral subsurface movement of relatively soft and mobile sediments in response to loading pressures exerted by the ice keel.

Deformation caused by ice keel overloading should range from simple load structures to more complex folded structures as seen in cores V-13 (Figure 4b, arrow 4), V-15 (Figure 6b, arrow 3), V-16 (Figure 7b, arrows 1 and 2), V-17 (Figure 8b, arrow 1), V-18 (Figure 9b, arrow 2), V-20 (Figure 11b, arrows 2 and 3), V-21 (Figure 12b, arrow 2), V-55 (Figure 16b, arrows 1 and 3), and V-76 (Figure 17, arrow 2). If an ice keel comes to rest on the bottom, simple loading will occur through the pressure exerted by the weight of the ice. The

resulting structures may be flame structures, ball and pillow structures or dish structures, seen in cores V-13 (Figure 4b, arrow 4), V-15 (Figure 6b, arrow 3), V-21 (Figure 12b, arrow 2), and V-55 (Figure 16b, arrow 1). If the grounded ice keel is subsequently moved, then a squeezing of the soft sediment below and away from the keel may occur and the result may be simple asymmetrical folds seen in cores V-16 (Figure 7b, arrow 1 and 2), V-17 (Figure 8b, arrow 1), V-18 (Figure 9b, arrow 2), V-20 (Figure 11b, arrows 2 and 3), V-21 (Figure 12b, arrow 3), V-55 (Figure 16b, arrow 3), and V-76 (Figure 17, arrow 2), pointing away from the bottom of the ice gouge, much like tooth paste squeezed out of a tube (Figure 21). Because the sediments are soft (fine grained and unconsolidated), the tendency for the material to flow is high and the result should be elongation (thickening) of the folds in the hinge area and thinning along the limbs (Billings, 1972). In actual cases of ice gouged sediments, a combination of loading and folding can be seen (Cores V-16 (Figure 7b, arrows 1, 2, and 3), V-17 (Figure 8b, arrow 1), V-18 (Figure 9b, arrow 2), V-20 (Figure 11b, arrows 2 and 3), V-21 (Figure 12b, arrows 2 and 3), V-55 (Figure 16b, arrows 1 and 3), V-76 (Figure 17, arrow 2 and 3).

The cores in this report provide examples of ice deformed sediments, however, the observer is limited to a 12 cm wide, unoriented cross-section through sediments that are known to be ice gouged. This makes the observation of large scale or continuous structures difficult. Figure 22 is a hypothetical cross-section through ice gouged sediments based on model considerations and cores. Figure 23 is a sketch of core V-16 from this study that might have been taken from an area not unlike Figure 22. Figure 24 is a photograph of a wider core taken through ice deformed sediments on the North Sea tidal flats and could also have been taken from an area of deformation modeled in Figure 22.

#### ICE-SEDIMENT INTERACTION

The cores analyzed in this study have offered a unique opportunity to observe the effects of ice sediment disturbance by drift ice on a high latitude shelf environment. The transect of cores intersects zones with different intensity of seabed disruption by ice. This situation has allowed us to observe the deformation of several depositional environments associated with varying degrees of ice-disturbed ocean bottom.

Figure 25 is a map of ice gouge intensity (a product of maximum gouge depth, maximum gouge width, and gouge density per kilometer) in the study area with the locations of the coring sites (after Barnes et al.,

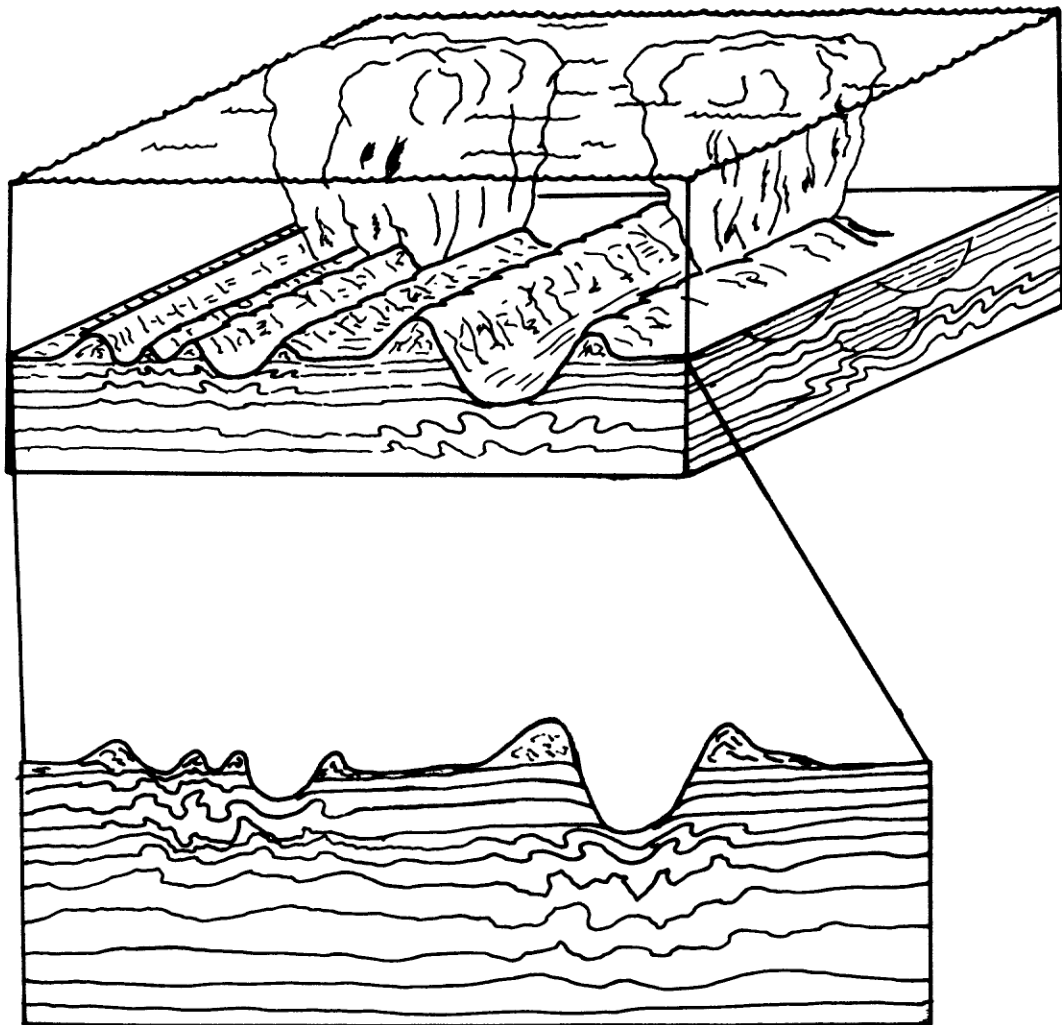


Figure 21. Schematic drawing of ice gouging process and related deformation of sea floor that may occur (modified after Barnes and Rearic, 1985). It is the author's belief that the sediments below the gouge would tend to flow away from the bottom of the gouge causing asymmetrical folds that are elongate (thickened) in the hinge areas and thin along the limbs, resulting in the apparent lengthening of lamina or bedding.

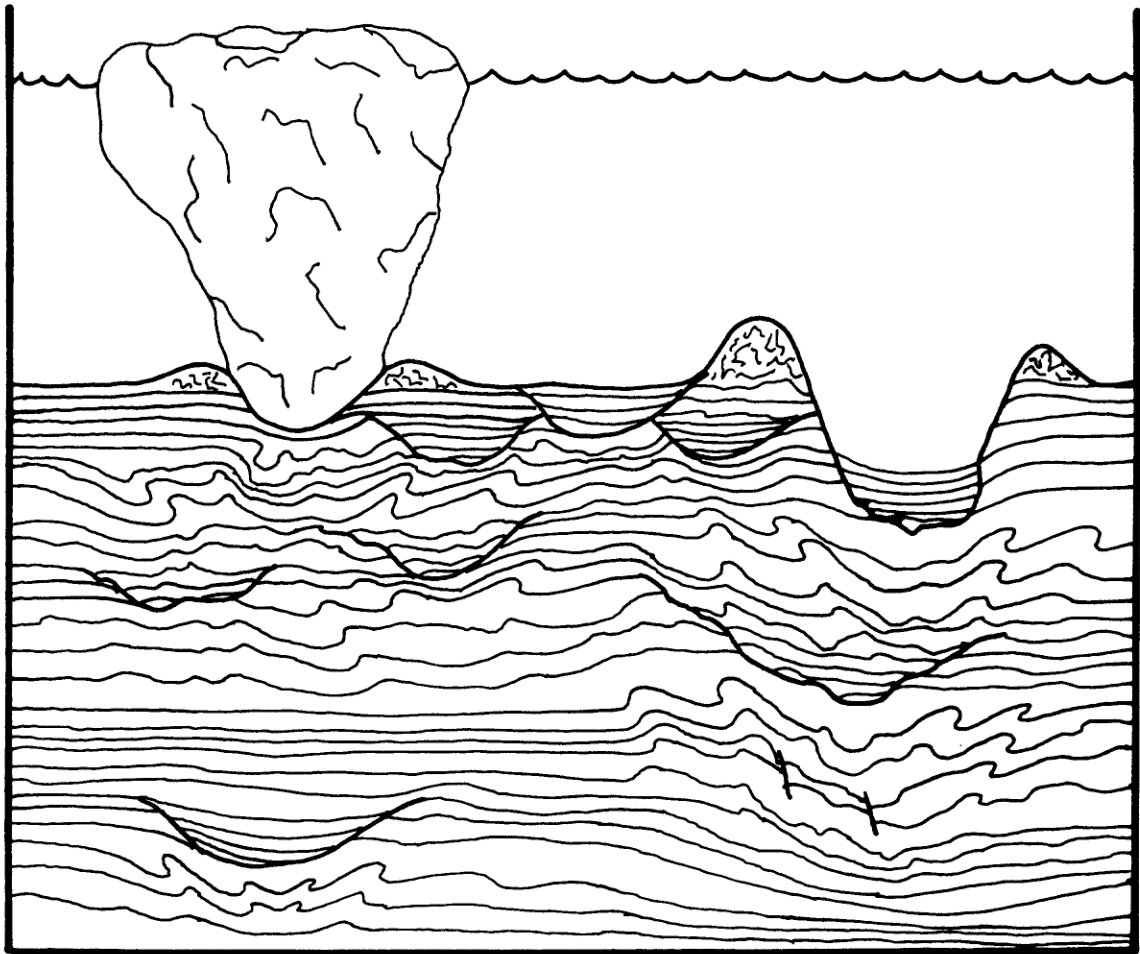


Figure 22. Schematic drawing of hypothetical cross-section through (preserved) ice gouged sediments. Heavy lines in cross-section are preserved gouge troughs. Refer to text for explanation.

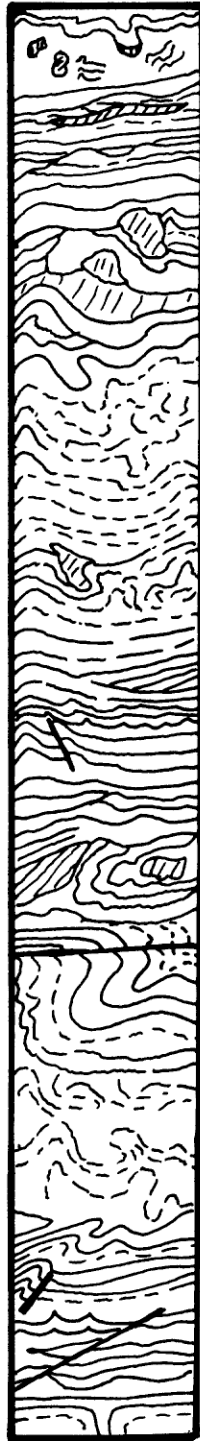


Figure 23. Sketch of core V-16, highlighting deformed zones in core. Compare this Figure with Figure 22 and Figure 24. Note similarity in deformational structures.



Figure 24. Photograph of ice deformed sediments from North Sea tidal flats. Note similarities to cores from study area. Scale is in centimeters. (Photo from Reineck and Singh, 1980).

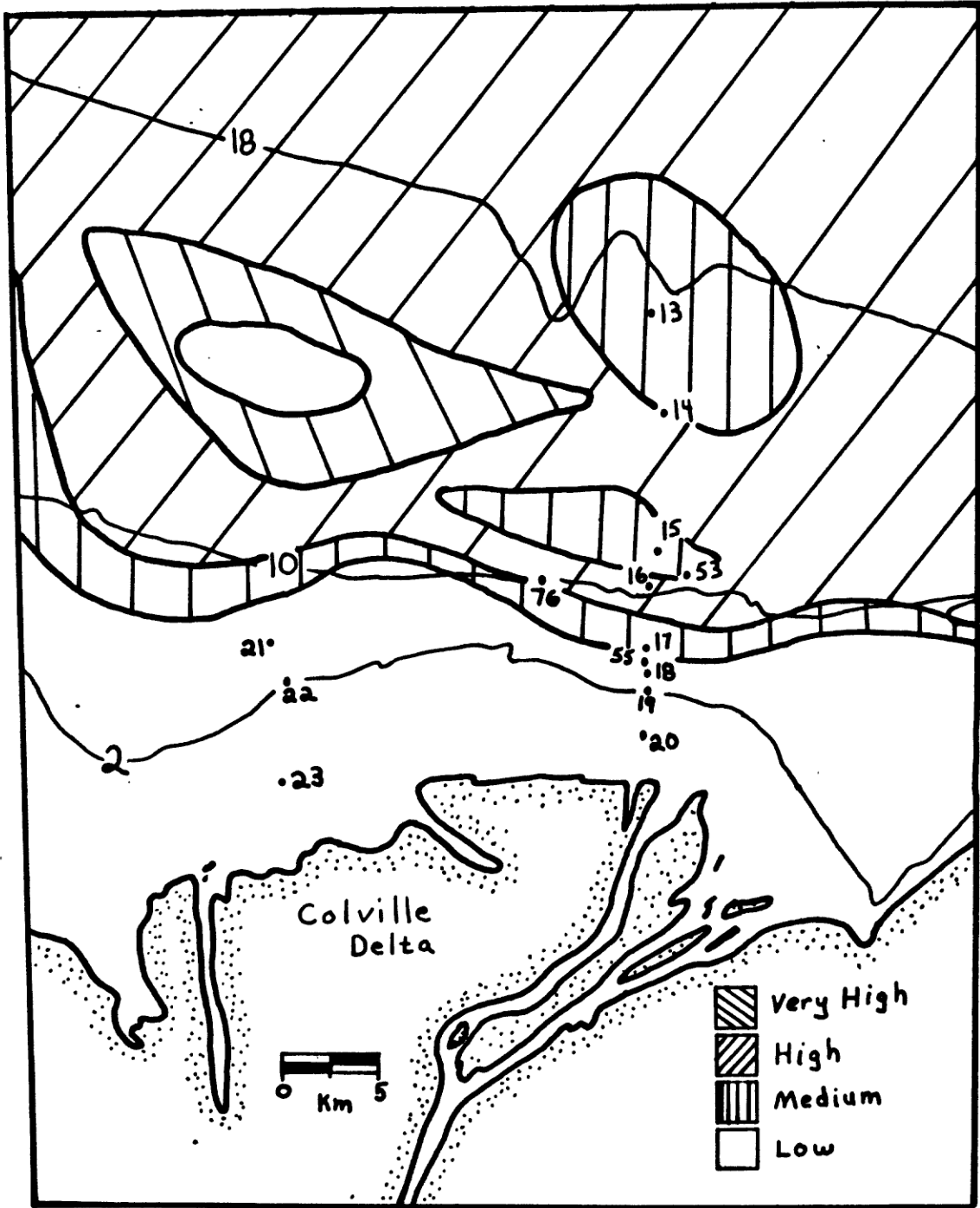


Figure 25 . Ice gouge intensity map with coring localities overlain (modified after Barnes et al, 1984). Note that core transect crosses several different mapped intensities of ice gouging. Refer to this figure throughout discussion of ice sediment interaction.

1984). It can be seen that gouge intensity is low shoreward of the 10m isobath (Barnes et al., 1984). Offshore of the 10 m isobath ice gouge intensity quickly increases and varies from medium to very high (Barnes et al., 1984).

The variability in ice gouge intensity has been related to variability in ice cover (Barnes et al., 1984). Onshore of the 10 m isobath is the zone of fast ice, an essentially stationary ice canopy that acts as an extension of the land (Reimnitz et al., 1978). Few winter gouges form in this area as ice movements are rare. At approximately the 10 m isobath, an inshore stamukhi zone forms during early winter where the stationary fast ice and the moving pack ice meet (Reimnitz et al., 1978; Barnes et al., 1984). Grounded first year pressure ridges develop at this boundary and actively scour the bottom as the pack rotates westward (Reimnitz et al., 1978; Barnes et al., 1984). Consequently the intensity of ice gouging increases at this boundary (Figure 25). Gouge intensity is variable and decreases slightly offshore of 10 m until approximately the 20 m isobath (Barnes et al., 1984) where the major stamukhi zone forms (Reimnitz et al., 1978). The grounded ice ridges of this stamukhi zone are believed responsible for the highest ice gouge intensities encountered on the shelf (Barnes et al., 1984). Intense gouging continues out to approximately the 40 m isobath and then decreases sharply because fewer ice keels can reach the bottom (Barnes et al., 1984).

Cores V-13 and 14 were taken from water depths of 19 m and 15 m respectively. Deformation in these cores is concave downward and is attributed to penetration of the core barrel (Figures 4b, arrow 3, and 5b, arrow 2). Small scale load features are present (Figure 4b, arrow 4) which is this author's belief result from overpressuring by grounded ice. In general, these cores show little ice-related deformation and this correlates with a decrease in ice gouge intensity in these water depths (Figure 25).

Cores V-15 through 17, 53 and 55 taken from the 13 m to 7 m depth range (Figure 1b), are believed to display intense deformation caused by ice gouging. Contorted and folded bedding, and loaded contacts are dominant. Rip-up clasts (Figures 6b, arrow 1, 7b, arrow 3, 8b, arrow 3) as well as truncated and offset bedding (Figures 7b, arrows 1 and 2, 8b, arrow 1, 16b, arrow 3) are present. In general, internal core stratigraphy is obliterated (Figure 7b). Here the intensity of possible ice related deformation cores corresponds to their position within the inshore stamukhi zone. The inshore stamukhi zone extends from approximately the 8 m isobath

to the 12 m isobath (Barnes et al., 1984), and cores extracted from this zone display the most intense ice related deformation. V-55 shows the smallest degree of deformation (visual estimate is less than 15% of core) of cores from this area and most likely lies just inshore of the most intense ice turbation.

With the exception of core V-20, cores V-18 through 23, all from water depths less than 4 m display little or no ice gouge related deformation. Internal stratigraphy within each core is coherent and consists dominantly of horizontally laminated sands, silts, and muds. These cores were extracted from the area that is covered by the fast ice canopy. It might be expected that little or no deformation is present in these cores, because there is little or no ice movement for most of the winter (Barnes et al., 1984), and any deformation may possibly be related to either shoreward ice push during winter, or to grounded ice during spring break-up. A few loaded contacts are present (Figure 9b, arrow 1, 11b, between arrows 1 and 2, 12b, arrow 2) but truncated laminations and bedding are probably related to hydraulic processes rather than ice. Core V-20 from 1.5 m of water and only 3 Km from the delta is the anomaly for this group of cores. A box fold is present in the upper half of the core (Figure 11b, arrow 2) and an overturned fold occurs in the lower half (Figure 11b, arrow 3). This author believes that these folds represent rare ice related disruptions.

If ice deformation of primary sedimentary structures occurs in the Beaufort Sea, as suggested by my observations, then ancient analogs of ice gouged sediments may be preserved in the stratigraphic record, and should be recognizable on the basis of their structural deformation. Two examples of environments from the literature known to have had floating ice present suggest the presence of ice gouged strata.

#### GLACIAL LAKE AGASSIZ: AN EXAMPLE OF PRESERVED ICE GOUGES

The preserved lake plain of former Glacial Lake Agassiz in southern Manitoba, eastern North Dakota, and western Minnesota around the Red River Valley displays a lake bed surface morphology that is characteristic of present day sea floor morphology in heavily ice gouged areas of the continental shelf off the north slope of Alaska (Clayton et al., 1965).

Lineations in the Lake Agassiz plain are typically characterized by ridges and troughs averaging 53 m wide and 2 m deep (Horberg, 1951) and bear a unique resemblance to ridges and troughs on the sea floor off the north slope of Alaska, where ridges and troughs are

typically 3 m wide and 1 m deep (Reimnitz and Barnes, 1974). In both instances, lineations may be as long as several kilometers.

Horberg (1951) was first to observe and characterize the ridges and troughs on the Lake Agassiz plain. Horberg hypothesized that the ridges were formed by either fracture filling between blocks of lake ice, or as tundra ridges due to grounded ice wedges. Colton (1958) stated that the ridges were the result of frozen ground structures formed during the retreat of the late Wisconsin ice sheet, and based his hypothesis on the occurrence of periglacial involutions, fossil ice wedges, and polygonal and network soil patterns. Clayton et al. (1965) reinterpreted the ridges and troughs as being ice-drag marks resulting from the grounding of floating (glacial) icebergs. Gerhard (1980) also interpreted the ridges to be the result grounded ice. Dredge (1981), Fenton et al. (1983), Mollard (1983), and others have interpreted the lineations present on the Lake Agassiz plain to be ice-drag features.

Horberg's earliest observations also documented the occurrence of deformation below ridges and troughs on the Lake Agassiz plain. His original description is as follows:

"Folded lake clays occur 3-8ft below the surface for a distance of about 25ft. Asymmetrical folds with dips up to vertical could be traced from one side of the ditch across its bottom to the other side. The largest fold has a height of at least 6ft. Other deformed zones a few hundred feet away are separated by areas in which the clay appears to be horizontal. At this locality it is difficult to explain the deformation other than by the former presence of grounded ice."

Fenton et al. (1983) documents the presence of preserved cut and fill structures and folds in the deposits of the Lake Agassiz plain. The cut and fill structures are believed to be preserved ice gouges below the present day surface, and the folds are believed to be a direct result of ice overloading. An outcrop sketch by Fenton et al. (1983) can be seen in Figure 26. Mollard (1983) presents the occurrence of large-scale folds and cut and fill structures for his hypothesis for the lineations being caused by ice scour.

The aforementioned surface morphology and structural features from the lake bed of Glacial Lake Agassiz are similar to those reported here from ice gouged sediments on the continental shelf off the North Slope of Alaska.

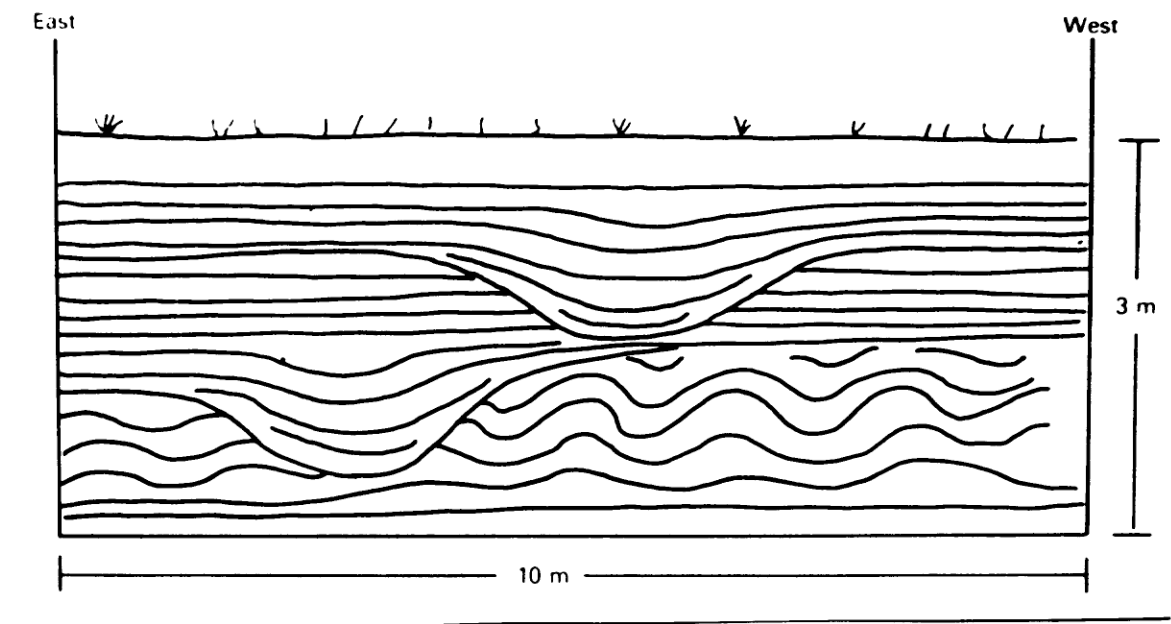


Figure 26. Outcrop sketch of preserved ice gouges and associated deformation from the Lake Agassiz plain. (From Teller and Clayton: eds. Fenton et al, 1983).

The documented occurrence of asymmetrical folds below the large cut and fill features on the Lake Agassiz plain by previous researchers supports my hypothesis for the type of deformation that may occur in the process of ice gouging. The similarities between the Beaufort Shelf surface morphology and core stratigraphy with Lake Agassiz surface morphology and sediments supports the interpretation that the features preserved in the Lake Agassiz plain are paleo ice gouges and that these features may be characterized on the basis of the sedimentary and deformational structures associated with them. The ability to trace lithologic units between ice gouges on the Lake Agassiz plain, in contrast to the lateral discontinuity in the Beaufort Sea, suggests a lower intensity of ice gouging, or more rapid sedimentation in Lake Agassiz. The lack of preservation of laterally continuous lithologic units in the Beaufort sea may reflect rapid reworking in relation to the rates of sedimentation.

#### LATE PLEISTOCENE LACUSTRINE SEDIMENTS OF THE ONTARIO BASIN, CANADA: AN ALTERNATIVE INTERPRETATION.

Glacial and postglacial sediments exposed in the cliffs along the Scarborough Bluffs at Lake Ontario, Canada consist in part of hummocky and swaley cross-stratified sands contained within a glaciolacustrine complex composed of fine grained sediments (Eyles and Clark, 1986).

The rocks, locally known as the Don Beds, represent sediments deposited on the floor of a glacier-dammed lake during early and middle Wisconsin time (Eyles and Clark, 1986). The sedimentary structures observed in the locality are described as subparallel undulatory cross-strata with low angle terminations and truncations that are either convex-up or concave-up defining a hummock or a swale respectively. The structures appear to be radially symmetrical and have wavelengths up to 4 m and heights up to 40 cm. Laminations along the top of the hummocky forms are typically truncated and mantled by symmetrical wave ripples and mud drapes. In many cases these bedforms are in erosional contact with similar bedforms above and below. These structures commonly contain ice-rafted dropstones and in some cases are reported to display convoluted and deformed bedding (Eyles and Clark, 1986). A typical outcrop and sketch can be seen in figure 27.

These deposits are interpreted to have formed as a result of sedimentation below storm waves that entrain large volumes of sand, and that hummocks may be very large post-vortex ripples with individual laminations representing pulses of liquefaction, suspension, and sedimentation of sand by a single storm wave or wave

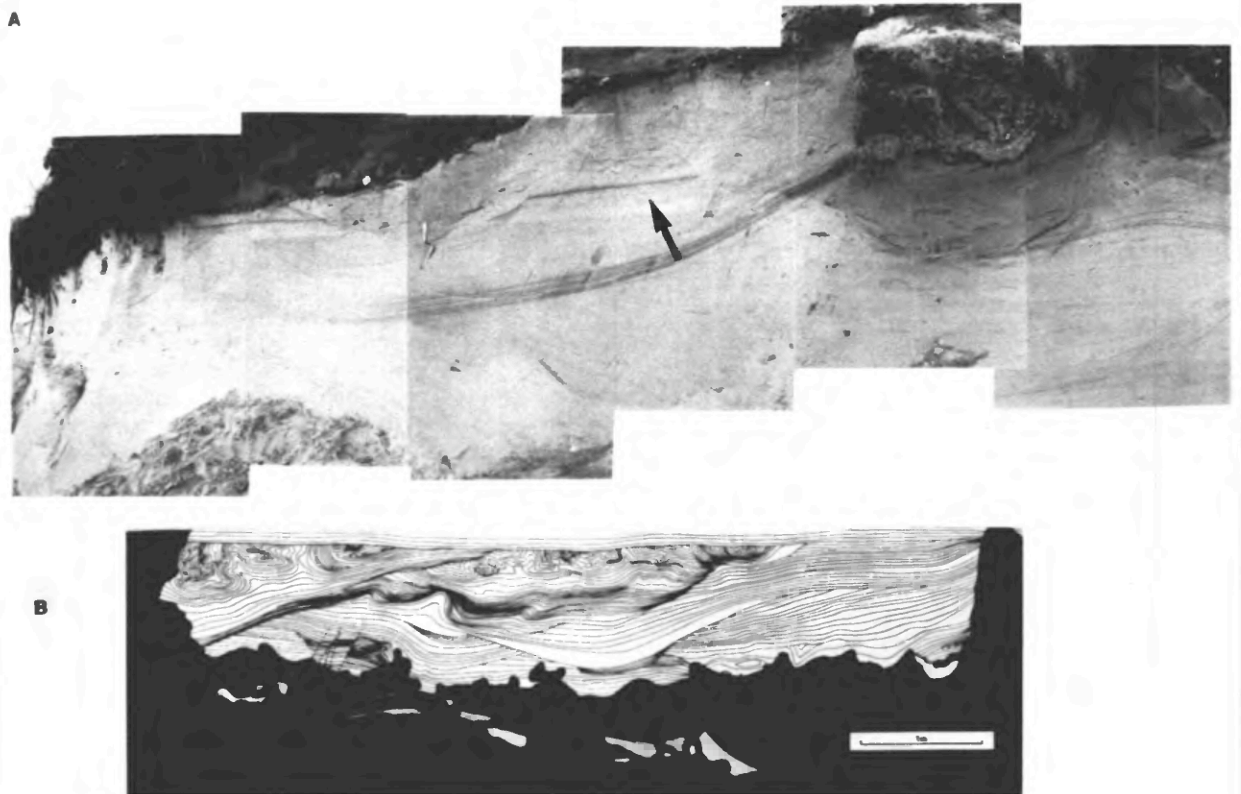


Figure 27. Outcrop photograph and sketch of believed storm generated bedforms in the Scarborough Bluffs, Ontario. Note the similarity to ice gouged sediments in Lake Agassiz (Figure 26), and compare to hypothetical cross section (Figure 22) and to structures present in cores (Figures 6, 7, 8, 9, 11, 12, 16, and 17). These unusual bedforms may very well be ice gouge related. (From Eyles and Clark, 1986)

train (Eyles and Clark, 1986). Eyles and Clark state that the precise hydrodynamic setting and evolution of such deposits are not fully understood, but believe that they must result from strong oscillatory flows, or at least oscillatory dominant combined flow (Eyles and Clark, 1986).

An alternative hypothesis for the development of the hummocky and swaley bedforms present in the Scarborough Bluffs suggests these structures may in part result from ice gouging. The paleoclimatic setting at the time of deposition of the units certainly favors the presence of floating ice, and is in part confirmed by the presence of dropstones.

The preservation of well defined cut and fill structures below which are deformed, laminated sediments, coupled with the presence of floating ice suggests the origin of these unusual structures could be related to drifting ice keels. It may be that some of these features are derived from storm generated waves, but the loaded nature of underlying contacts, and the deformed character of the sediments involved, as well as the similarity to described localities of known ice gouged sediments (Fenton et al., 1983), give strong evidence in favor of ice disrupted sedimentation in the area.

---

## SUMMARY

The relative intensity of disturbance caused by grounded ice seen in a transect of sediment cores can be directly correlated to patterns of mapped ice gouge intensity in the same area, and the ice gouge intensity can subsequently be correlated to areas of greatest pressure ridge development.

A hypothetical model based on the sedimentological characteristics of cores in this study has been developed for the deformation associated with the ice gouging process. Soft sediment deformation in areas where ice gouging is dominant is believed to range from simple load structures to more complex folded and faulted bedding. This deformation has been depicted schematically in a hypothetical cross-sectional model (Figures 21 and 22).

The data gathered in this study have been compared to ancient rocks from areas where floating ice was known to be present. Deformation in sediments documented in the ancient environment correlates to deformation observed in the modern analog and is believed to fit the hypothetical model.

Furthermore, sediments and structures in the Ontario Basin believed to have been derived from storm generated currents have been compared to cores and observations in this study. An alternative interpretation of those sedimentary structures proposed here is that they are the result of sediment disturbance by drifting ice.

## CONCLUSIONS

The sediments investigated in this study have a complex depositional history that has in many cases been overprinted by deformation caused by the process of ice gouging. The fact that ice-sediment interaction plays an important role in the development of deformational structures is evident from the cores analyzed in this study.

1. Ice related deformation has been preserved in recent sediments from the study area.
2. Ice related deformation can range from simple load structures to complex folded and faulted structures.
3. The intensity of ice related deformation can be tentatively correlated with mapped trends in ice gouge intensity.
4. Lithologic, textural, and structural criteria

normally used to classify sediments to a depositional environment may be entirely obliterated if ice was present during deposition or prior to lithification. Areal extent of one laterally continuous lithologic unit is probably greatly influenced by the relative intensity of the ice gouging process.

5. Deformational features found in ice gouged sediments are unusual enough to be used as a base criteria for the identification and interpretation of ancient ice-deformed sediments, and two examples have been used to illustrate and support this argument.

This has been a preliminary investigation; in-depth experiments on the formation of ice related deformation, and exhaustive field work to find more examples in the stratigraphic record have not been conducted. Emphasis in future studies should be concentrated on working laboratory models of ice gouging, and extensive field work should be conducted to ascertain if other examples of preserved ice gouges and the associated deformation exist in the ancient rock record.

## APPENDIX A

### CORE DESCRIPTIONS

#### CORE V-13B

Core V-13B located at 70°44.8" north latitude, 150°28.1" west longitude in 19 m of water.

0-10 cm is composed of clay, green to green gray, massive, burrows and pelecypod fragments present. Sand interbeds and laminae scattered with contorted contacts. Sand is pink, clear, and translucent, fine to very fine grained quartz. Hematite (limonite ?) staining common in sand.

10-16 cm is sand, pink, clear, and translucent quartz, commonly with Fe oxide stain, fine to very fine grained, scattered medium grains and shell fragments. Mud balls common in this unit, composed of green to gray clay.

16-19 cm is sandy clay, green to green-gray, pelecypod fragments common, upper and lower contacts deformed.

19-25 cm is clay and sand interbeds. Clay is green to green-gray, massive, slightly mottled, sand is fine to very fine grained clean quartz. Bedding and contacts very irregular and contorted, deformed.

25-39 cm is clay, green to green-gray, sandy in part with shell fragments common, massive, upper contact deformed.

39-49 cm is sand, pink, clear, and translucent, fine to very fine grained quartz, horizontally

laminated, upper and lower contacts deformed, loaded.

49-51 cm is sandy clay, massive, upper and lower contacts deformed.

51-53 cm is clay, green to green gray, massive, deformed contacts.

53-59 cm is sandy clay, visibly laminated in upper 4cm, laminations slightly deformed, some possibly truncated, lower 2 cm is massive.

59-61 cm sand lense extending upward at 30 degrees and in 3 cm into sandy clay, contacts irregular.

61-76 cm is sandy clay, scattered coarse sand grains and pebbles, rare pelecypod fragments, some distorted laminations in upper part, slightly mottled with irregular pockets of sand or pebbly mud. Lower contact visibly deformed.

76-87 cm is composed of interbedded clay and sandy clay, laminations well defined, and in places highly deformed, very tight recumbent fold in the middle of this section, deformation may be a result of coring disturbance.

#### CORE V-14

Core V-14 located at 70°41.5" north latitude, 150°27.2" west longitude in 15 m of water.

0-9.5 cm is composed of silty sandy clay, slightly mottled, no distinct bedding, brown to brownish-gray.

9.5-11.5 cm is composed of sand, fine to very fine grained with abundant pelecypod fragments and pebbles. Upper and lower contacts deformed, (loaded?).

11.5-63.5 cm is composed of clay, dark to drab green, and brown, silty in spots but with random orientation, massive in core and peel, faint bedding and laminations visible in radiograph, highly deformed in spots, some actual offset observed in laminations on radiograph. Slight edge deformation due to coring.

Overall character of core is coarsening upward.

#### CORE V-15

Core V-15 located at 70°37" north latitude, 150°27" west longitude in 12.4 m of water.

0-9 cm is composed of sand, fine to very fine grained with silty matrix, no visible bedding in core or peel, but large burrow evident on radiograph from 0 to 4 cm. Burrow has cleaner sand of same grain size. Sand is relatively homogeneous with cleaner sand in lower part. Lower contact is highly deformed.

9-14 cm is clay, gray to green, massive, very sandy in part (pockets?). Upper and lower contacts deformed.

14-18.5 cm is sand, fine to very fine grained, silty matrix, laminated, with some laminations truncated

just below upper contact.

18.5-20.5 cm is a lense of clay, green to gray and massive.

20.5-23.5 cm is sand, fine grained and admixed with sandy clay, moderately well laminated, some shell fragments present, upper contact with clay lens is highly deformed (loaded), lower contact only moderately deformed.

23.5-25 cm is a lens of clay, green to gray, massive.

25-29.5 cm is sandy clay, gray to greenish, some laminations visible on radiograph near top contact, moderately deformed, shell fragments visible on radiograph and in core.

29.5-31 cm is sand, very fine grained, silty matrix, upper and lower contacts highly deformed.

31-41 cm is clay, gray to green, massive, some laminations evident in lower part, all laminations are deformed giving a distinct mottled appearance on the radiograph, laminations not visible on core, but are faint on peel.

41-44.5 cm is sand, fine to very fine grained, moderately well laminated, possible ripple cross laminations in upper part. Upper contact also deformed.

44.5-46.5 cm is sandy clay, gray to greenish, grading into sand in lower part.

46.5-50 cm is sand, fine to very fine grained, silty in top part grading into clean sand in bottom, steep angular cross laminations are truncated at upper contact. Large block of moderately clean sand is apparent on radiograph, however the same area appears only deformed on peel. Laminations in block are horizontal.

50-51.5 cm is clay, green to greenish gray, massive, upper and lower contacts highly deformed.

51.5-55.5 cm is sand and sandy clay, clay pockets present, highly irregular and deformed upper and lower contacts.

55.5-62.5 cm is clay and sandy clay, green to gray and dark gray, massive except where very sandy, two 1x4cm blocks of sandy clay are visible on the radiograph in the middle of this section. Blocks are well laminated and rest together with great angular discontinuity, upper contact highly deformed, lower contact slightly deformed.

62.5-77.5 cm is sand and sandy clay, sand is very clean, dark gray, and appears to be tightly folded, very fine grained. The sandy clay occupies the inside of the fold. The sand also contains scattered pebbles and shell fragments.

77.5-97.5 cm is composed of highly deformed sandy

clay and silt, gray to dark gray, sand is very fine grained. Some sandy pockets. Deformation appears to be the result of core removal.

#### CORE V-16

Core V-16 located at 70°36.3" north latitude, 150°28.2" west longitude in 11.5 m of water.

0-5 cm is clay, dark green to drab, massive in core, some bedding in peel, appears mottled on radiograph. Sandy in part with sand occurring in small pockets.

5-47 cm is clay, sandy clay and sand laminae. Clay is dark green to brown, massive in core and peel, laminated in radiograph. Sandy clay is green to gray in core, gray in peel, massive in core, some structure is evident in peel, laminated in radiograph. Sand is fine to very fine grained quartz with silty matrix, massive in core, laminated in peel and radiograph. This portion of core is extremely disrupted and deformed. Deformation is best explained by coring effects since much of the greatest deformation occurs at core edge.

47-50 cm is sand, brown to gray, fine to very fine grained, laminated, deformed.

50-62 cm is clay and sandy clay. Clay is dark green to brown, and gray, mottled in core and peel, laminated and deformed in radiograph. Sandy clay is green to gray in core and peel, laminated in core and peel, laminated and deformed in radiograph. Upper and lower contacts of this unit are deformed.

62-97.5 cm is composed of clay and sandy clay with sand pockets. Clay is green to gray, massive in core, laminated in peel and radiograph. Sandy clay is light to dark gray, massive in core laminated in peel and radiograph. This section of core is extremely deformed. Some small scale folds exist as well as numerous shear planes and offset laminations. Folds and offset are best visualized on radiograph. Deformation is probably not coring related as some overlying units are relatively undeformed.

#### CORE V-17

Core V-17 located at 70°34" north latitude, 150°28.2" west longitude in 8.5 m of water.

0-10 cm is clay, dark green, massive in core, but slightly silty in part, vertical structure visible in radiograph may be a relic burrow or some type of coring disturbance.

10-10.5 cm is a lens of light gray, fine grained sand, appears to be the terminating point of vertical structure mentioned above.

10.5-20.5 cm is clay, dark green, massive, with very fine grained, laminated silty sand pockets. Laminations in sand pockets are deformed.

20.5-23.5 cm is clay, dark green, massive, some contorted laminations visible on radiograph.

23.5-24 cm is sand, light gray, very fine grained, silty, deformed.

24-40.5 cm is clay, dark green, massive in core and peel, highly deformed in radiograph, sandy in part, scattered pelecypod and gastropod shell fragments.

40.5-47.5 cm is clay and sandy clay. Clay is green to gray, faint bedding in core and peel, deformed in radiograph. Sandy clay is gray, laminated in core and peel, highly deformed in radiograph. This unit grades down into sand and clay interbeds.

47.5-62.5 cm is sand and clay interbeds. Sand is gray, fine to very fine grained, laminated. Clay is green to gray, mostly massive but mottled in part. This unit has a highly mottled appearance due to the highly contorted nature of the sand/clay lamination contacts. Some deformed lenses of sand are also present.

62.5-67.5 cm is sand, gray, very fine grained, silty, deformed.

67.5-74.5 cm is clay, dark green to gray, massive to horizontally laminated, some contacts deformed.

74.5-79.5 cm is sand, fine to very fine grained, very silty matrix, laminated. Two small blocks of this material rest inside this unit with an angular discontinuity of laminations, and appear to be blocky intraclasts or rip up clasts.

79.5-82.5 cm is clay, green, faintly laminated, deformed.

82.5-84.5 cm is interbedded very fine sand and silt, and clay. Laminations in this unit are deformed and sheared, and offset is apparent on radiograph. Contacts highly deformed.

84.5-95.5 cm is composed of interbedded clay and sandy clay. Appears massive in core, some bedding in peel. Laminated and deformed on radiograph. Small folds and shear plane with offset are visible in bottom of core on radiograph.

#### CORE V-18

Core V-18 located at 70°33.2" north latitude, 150°27.9" west longitude in 3.3 m of water.

0-17 cm is composed of sand and clay interbeds. The sand is gray, fine to very fine grained, partially oxidized, horizontally laminated. The clay is medium to light gray, silty in part, horizontally laminated. Slight edge deformation due to coring.

17-18 cm is clay, gray, massive in core, laminated

in peel and radiograph, upper contact deformed.

18-22 cm is clay, sandy clay, and sand interbeds. Sand and clay as above, horizontally laminated.

22-23 cm is sand, gray, very fine grained, ripple cross lamination which are truncated at upper contact.

23-25 cm is clay, greenish gray, massive.

25-26.5 cm is sand and organic interbeds. Sand is gray, fine to very fine grained, lenticular with laminations truncated against edge of organics. Organics a light to dark brown and black, fibrous plant material and detritus, lensoidal.

26.5-28.5 cm is sand, gray to light gray, fine to very fine grained, silty, horizontally laminated with some laminations approaching crossbedding, erosional upper contact with unit above, markedly angular.

28.5-32 cm is sand and organic (peat) interbeds. Sand is as above but truncates horizontally laminated organics. Organics consists of partially oxidized compacted fibrous plant debris.

32-40.5 cm is horizontally laminated sand, clay, and organic interbeds. The sand is gray, fine to very fine grained, disseminated organic component to grains, silty in part, horizontally laminated. Clay is green to gray, faintly laminated, rich in organics, some wholly organic laminae.

40.5-41 cm is peat, horizontally laminated with slightly deformed lower contact.

41-41.3 cm is clean sand, very fine grained, horizontally laminated.

41.3-43.3 cm is peat, green to dark brown and black, some coal possible, horizontally laminated, highly deformed lower contact.

43.3-50 cm is clay with minor sand and organic interbeds. Clay is green to gray, massive in core, faintly laminated in peel and radiograph. Organic content of clay is high (25-30%) and is very visible on radiograph.

50-51 cm is sand, gray, fine to very fine grained, silty, ripple cross laminated. Cross laminations are truncated along upper contact.

51-55 cm is sand, light gray, fine to very fine grained, silty matrix, horizontally laminated with abundant organics. Organic laminations truncated by sand body.

55-56 cm is clay, greenish gray, massive, grading downward into sandy clay and clay.

56-59 cm is clay and sandy clay with minor interbedded organics and sand pods. Clay and sandy clay is green to gray, slightly mottled, horizontally laminated, small organic component. Small sand pods are fine grained, silty, well laminated, and show up on radiograph as well laminated blocks and angular chunks

suspended in the clay.

59-77 cm is clay, dark green to gray, massive in core, well laminated on radiograph. Some lamination contacts show minor deformation (loading?), minor organic component.

77-78 cm is peat, green to brown and black, some coal possible, compacted, well laminated.

78-111 cm is clay and sandy clay. Clay is green to green gray, massive in core and radiograph, minor organic component, appears highly bioturbated on radiograph but no burrows can be discerned. Clay grades downward into sandy clay. Sandy clay is gray, massive, also appears bioturbated, but no burrows evident. Sandy clay in this unit grades to clayey sand along its bottom contact. Obvious overall fining upward sequence.

111-112.5 cm is clay, greenish gray, massive, deformed upper and lower contacts.

112.5-119.5 cm is sand, gray, fine grained, silt and clay matrix, high organic content, massive.

119.5-166 cm is composed dominantly of clay with one large structure in it composed of sand and organics. The sand is gray, fine grained and interbedded with compacted fibrous plant debris, (grasses?). The structure forms a partial fold with the laminations being vertical in relation to the core at the top of the structure, and tapering off to about 30 degrees in the bottom part of the structure. This structure is suspended in a body of clay and has no similar lithologies above or below it. The clay surrounding this structure is green to gray, massive in core and radiograph, but has a high organic content that appears to be rootlets of grasses and plant stems. The organics incorporated into the clay do not form any crude bedding, but do, however, appear to be in growth position. There is also no evidence of bioturbation in this section, but it is highly suspect.

#### CORE V-20

Core V-20 located at 70°31.4" north latitude, 150°27.5" west longitude in 1.5 m of water.

0-9.5 cm is composed of sand, brown to dark brown, oxidized, fine to very fine grained, horizontally moderate to well laminated.

9.5-10.5 cm is sand, medium to dark brown, fine to very fine grained, interbedded with fibrous organic matter, ripple cross laminated with cross laminations truncated along upper contact.

10.5-15 cm is sand, dark gray to brown, fine grained, silty, interbedded with organic debris and coal, horizontally laminated. Organic matter is a

component grain in the sand.

15-26 cm is sand, clay and organic interbeds. The sand is light gray, fine grained, has a silt and clay matrix, horizontally laminated. Clay is green to gray, massive in core, faintly laminated in peel, well laminated in radiograph. The organic laminae are dark brown to black, well laminated fibrous organic matter.

26-40.5 cm is sandy clay interbedded with organics. The sandy clay is gray, with fine to very fine sand, well laminated with dark brown fibrous organic interbeds. This section of core is highly deformed into a box fold like structure. The structure is most visible on the peel, but does show up on the radiograph. The structure is concave up and is most likely not the result of coring.

40.5-47.5 cm is clay and organic interbeds. Organic interbeds in this section are large and average 1 cm in thickness, are brown, and have a large coal component. All laminae in this section are affected by deformation in unit above, and show a concave up structure.

47.5-59.5 cm is sand, gray to brown, fine to very fine grained, some organic component and interbeds, highly deformed laminations.

59.5-70.5 cm is of sand and clay interbeds. The sand and clay is as above, but the interbeds are highly deformed into a structure that resembles a recumbent fold. The fold is truncated along a shear plane just upwards of its axis, and holds a great resemblance to a thrust plane. This structure is extremely well defined in both the peel and radiograph.

70.5-87.5 cm is sand, gray to brown, fine to very fine grained, massive with a distinct mottled appearance on core, peel and radiograph. This section shows many irregular truncated planes and appears highly deformed, although no consistent lamination planes are present.

87.5-122.5 cm is composed of sand, sandy clay, and silt and organic interbeds. The sand and sandy clay occupy the upper 3 cm of this unit and are medium to light gray with very fine grained sand, moderately laminated with little deformation. This sandy clay grades down into silt, green to gray, and brown, with dark brown fibrous organic interbeds. This unit is moderately well laminated and shows no deformation other than edge effect due to coring. Several sets of asymmetrical ripple marks with cross lamination exist with the cross laminations on all sets being truncated along their upper contact.

CORE V-21

Core V-21 located at 70°33.8" north latitude.

151'.01" west longitude in 4 m of water.

0-1 cm is composed of clay, light gray, massive.

1-36 cm is sand, light brown to gray, fine to very fine grained, silty matrix, well laminated, highly deformed, scattered clayballs. This unit is highly deformed, with a structure resembling a large fold in the top 15 cm. Laminations around clay bodies show evidence of flow, minor folds throughout unit. Faint vertical burrow can be seen on radiograph.

36-37 cm is clay, gray, massive.

37-38 cm is sand, medium gray, fine grained with silty matrix, well laminated, slightly deformed.

38-41 cm is clay, sand, and organics. Clay and sand as above, organics are light brown to brown and black, some coal evident, well laminated.

41-68 cm is clay, green to gray, massive, partially mottled on radiograph.

68-70 cm is sand, gray, fine to very fine grained, poorly laminated, highly deformed upper and lower contacts (loaded?).

70-72 cm is clay, greenish gray, mostly massive with some mottled texture in radiograph.

72-77 cm is sand, fine grained, silty matrix, some lamination apparent on radiograph, highly deformed lower contact.

77-83 cm is clay and sand interbeds. Clay is gray to green, and massive. Sand is gray, fine grained, very silty, faintly laminated, lensoidal.

83-91.5 cm is clay, green to gray, massive with some sandy pockets.

91.5-92.5 cm is sand, gray, fine grained, silty, faintly laminated, upper and lower contacts slightly deformed.

92.3-93.5 cm is clay, gray, massive.

93.5-96 cm is sand, gray to brown, fine to very fine grained, silty, faintly laminated, lensoidal.

96-117 cm is clay, gray, partially laminated in upper and lower part, mottled to massive in remainder. Upper and lower contacts slightly deformed.

117-119 cm is sand, gray, fine grained, silty, massive, upper and lower contacts deformed, with lower contact highly deformed.

119-121 cm is clay, gray to green, massive. Upper contact highly deformed, lower contact undeformed.

121-122 cm is sand, gray, fine grained, silty, massive.

122-137 cm is clay, greenish gray, mostly massive but has some evidence of faint laminations in upper and lower part on radiograph, some minor shell fragments.

137-140 cm is sand, gray, fine to very fine grained, silty in part, well laminated, highly deformed, may be partially folded.

140-155 cm is clay, green to gray, massive, some evidence of faint laminations on radiograph, highly deformed upper and lower contacts.

155-157 cm is clay with abundant organics. Clay is gray, and massive. Organics are disseminated peat and plant stems or small twigs?.

157-177 cm is composed of clay (as above) with small organic rich pockets and interbeds. Moderately laminated with some deformation along lamination contacts.

#### CORE V-22

Core V-22 located at 70°32.5" north latitude, 150°59.6" west longitude in .6 m of water.

0-12 cm is composed of silty sand, medium to light gray, fine to very fine grained, scattered shell fragments and mudballs, faintly laminated.

12-87 cm is sand with intermixed organics. The sand is brown to dark gray, fine to very fine grained, very silty, high organic component as grains (coal), well laminated, highly deformed. Organic interbeds are very fine fibrous plant debris, compacted, well laminated, deformed. This unit shows an unusual structure in its middle. The structure is composed of steeply dipping laminations dipping in different directions about a central axis. Near the central axis the laminations dip less and approach horizontal. Several ripple cross lamination sets are prevalent in this unit, and are subsequently deformed by this structure. Below this structure is undeformed horizontal laminations.

87-88 cm is clay, green, massive, with some shell fragments.

88-98 cm is sand, brown to gray, fine to very fine grained, silty, small organic component, horizontally laminated.

98-114 cm is sand and clay interbeds. The sand is brownish gray, fine grained, silty, faintly laminated, deformed. The clay is gray, generally massive but with some faint lamination, laminated in radiograph.

114-170 cm is composed of sand, clay, and organic interbeds. The sand is gray to brown, fine to very fine grained, very silty in part, horizontally moderately to well laminated, high organic component to grains, several sets of ripple cross lamination apparent. The clay is gray, massive with a moderate organic component. The organics are well laminated, highly abraded plant debris and coal, including twigs, grasses, plant stems, and peat. One organic rich lamination contains a twig 1 cm in diameter. A vertical burrow 45 cm long is present in this unit and can easily be seen on the radiograph as

well as the peel. The burrow has caused little to no disturbance of the laminations that it penetrates.

#### CORE V-23

Core V-23 located at 70°29.5" north latitude, 150°59.5 west longitude in 1 m of water.

0-4 cm is composed of sand, brown to gray, fine to very fine grained, silty, horizontally laminated.

4-7 cm is clay, green, massive.

7-8 cm is sand, gray, clean, oxidized, fine grained, horizontally laminated.

8-10.5 cm is clay, greenish gray, faintly laminated, some fine sand laminations.

10.5-15.5 cm is sand, brown to gray, fine to very fine grained, silty, horizontally laminated with undulating contacts.

15.5-34.5 cm is clay and organic interbeds. The clay is greenish gray, and massive. The organics are brown to black, very fine, fibrous, horizontally laminated.

34.5-44.5 cm is sand, medium to fine grained, mottled, bioturbated?, faintly deformed laminae.

44.5-48.5 cm is clay and sand interbeds. Clay as above, sand is gray fine grained, silty, laminated.

48.5-51.5 cm is clay and organic interbeds. Clay as above, organics are thin fibrous laminae of plant detritus.

51.5-52 cm is sand, gray, fine grained, silty, ripple cross laminated to horizontally laminated.

52-57 cm is clay, organics, and minor sand laminae. Clay, sand, and organics as above, horizontally laminated.

57-61 cm is sand, gray, fine grained, silty, several ripple cross laminated set with laminations truncated along top contacts of individual sets. Appear almost as climbing ripple marks.

61-73 cm is clay, greenish gray, massive to horizontally laminated, minor organic component.

73-74.5 cm is sand, gray, fine grained, silty, massive.

74.5-96.5 cm is sand and organic laminae. The sand is gray, fine grained silty, well laminated. The organic matter is composed of brown fibrous plant detritus, rootlets, stems and twigs. This unit is dominantly ripple cross laminated with the cross laminations reflected in the organics as well as the sand. Most of the cross lamination sets are truncated along the upper contacts. The bottom most 5 cm of this unit is horizontally laminated.

96.5-144 cm is composed of clay and organic interbeds and laminations, with minor sand laminations.

The sand, clay and organics are as above, but this unit is dominantly horizontally laminated. Some ripple cross lamination does occur in the small sand bodies and in some of the organics.

#### CORE V-53

Core V-53 located at 70°36.69" north latitude, 150°24.8" west longitude in 13 m of water.

0-6.5 cm is composed of clay, greenish gray, highly mottled, bioturbated?, some shell fragments and pebbles.

6.5-19.5 cm is sand, gray, fine grained, well laminated with abundant shell fragments in lower part, upper contact deformed.

19.5-21.5 cm is clay, green gray, massive with distorted (loaded?) lower contact.

21.5-28 cm is sand, gray, fine grained, silty, oxidized in part, horizontally laminated.

28-73 cm is clay to sandy clay, mostly massive, but where sandy shows laminations. Some ripple cross lamination present, highly deformed in part, some shell (pelecypod) fragments present.

73-84 cm is composed of sand and clay. The sand is gray, fine to very fine grained, silty, laminated, highly deformed. The clay is greenish gray, sandy in part, laminated, deformed. This unit displays a highly deformed structure in its center. The structure is composed of sand and shows the flow features around its boundaries and in the clay. This was most likely produced by coring.

#### CORE V-55

Core V-55 located at 70°33.88" north latitude, 150°28" west longitude in 7 m of water.

0-10 cm is composed of clay, greenish gray, massive to mottled, deformed.

Next is 3 cm of sand, gray, fine to very fine grained, silty to clayey, laminated.

10-16 cm is clay, greenish gray, massive to faintly laminated, slightly deformed.

16-24 cm is sand, medium to light gray, fine to very fine grained, silty, horizontally laminated, lower contact highly deformed.

24-49 cm is clay, gray, massive to mottled, some parts faintly laminated, bioturbated, slightly deformed.

49-50 cm is sand, gray, fine to very fine grained, silty, horizontally laminated, lensoidal.

50-84 cm is clay, green gray, massive to faintly laminated, bioturbated?, Highly deformed in lower part

of unit with some folding evident.

84-88.5 cm of sandy clay and organic interbeds. The clay is gray, and massive. The organics are brown to brown-black, fine grained fibrous plant detritus, and peat. This unit shows some moderate deformation.

88.5-124.5 cm is clay, green gray, massive to mottled and faintly laminated, bioturbated?, some minor interbeds and pockets of fine sand, deformed.

124.5-154.5 cm is sand and clay interbeds. The sand is brownish gray, fine grained, silty, laminated, slightly deformed. The clay is green gray, massive to faintly laminated, slightly deformed.

#### CORE V-76

Core V-76 located at 70°37" north latitude, 150°34.8" west longitude in 10.7 m of water.

0-55 cm is composed of sand, gray, medium to fine grained, silty in part, well laminated, deformed. This unit shows a great deal of deformation. The upper portion of this unit displays a dominant concave up moderate deformation. The lower portion of this section displays steeply dipping to partially folded laminations which show some evidence of flow along lamination interfaces, highly deformed. The two different types of deformation are distinctly different and the lower set of deformed laminations is truncated at the top by the upper set.

55-66 cm is clay, gray to gray-black, partially oxidized, highly mottled, with abundant pelecypod fragments and some complete half shells.

66-91.5 cm is sand, gray, fine grained, very silty, horizontally well laminated to deformed well laminated. The upper portion of this unit is composed of horizontally well laminated silty sand. The lower portion of this unit is composed of horizontally well laminated sand that has been deformed into a concave up low amplitude fold. The laminations along the upper contact in the lower part are truncated and the contact is visibly dipping. Everything above the contact is horizontally well laminated and undeformed. A large clay block (containing organics) 3x3 cm sits directly on the contact between the two parts of this unit.

91.5-96.5 cm of clay, gray to gray-black, highly mottled with a large gastropod shell visible in the radiograph, bioturbated.

96.5-112.5 cm is sand, gray, fine grained, silty, massive, deformed lower contact, some small mud pockets.

112.5-115 cm is clay, gray to gray-black, faintly laminated, deformed upper and lower contacts.

115-123.5 cm is sand, gray, fine grained, silty,

laminated, deformed upper and lower contacts.

123.5-137 cm is composed of clay, gray to gray-black, massive to faintly laminated with several ripple cross laminated fine grained silty sand stringers, slightly deformed.

## REFERENCES

- Barnes, P.W., Rearic, D.M., and Reimnitz, E., 1984, Ice Gouge Characteristics and Processes: in The Alaskan Beaufort Sea: Ecosystems and Environments. Barnes, P.W., Schell, D.M., and Reimnitz, E., eds. pp. 185-212.
- Barnes, P.W. and Rearic, D.M., 1985, Rates of Sediment Disruption by Sea Ice as Determined from Characteristics of Dated Ice Gouges Created Since 1975 on the Inner Shelf of the Beaufort Sea, Alaska: U.S. Geologic Survey Open-File Report 85-463, 35pp.
- Barnes, P.W. and Reimnitz, E., 1972, River Overflow onto the sea ice off the northern coast of Alaska, spring 1972: Transactions, American Geophysical Union, 53:1020.
- Barnes, P.W. and Reimnitz, E., 1973a, New Insights into the influence of ice on the coastal marine environment of the Beaufort Sea, Alaska. Symposium on Significant Results Obtained from the Earth Resources Technology Satellite, Volume 1, Technical Presentations, Section A, Paper No. M7, pp. 1307-1314.
- Barnes, P.W. and Reimnitz, E., 1973b, The shore fast ice cover and its influence on the currents and sediments along the coast of northern Alaska: Transactions, American Geophysical Union 54:1108.
- Barnes, P.W., Reimnitz, E., Gustafson, C.W. and Larsen, B.R., 1973, U.S.G.S. marine studies in the Beaufort Sea off northern Alaska, 1970-1972: U.S. Geologic Survey Open-File Report 561, 11pp.
- Barnes, P.W., and Reimnitz, E., 1974, Sedimentary Processes on Arctic Shelves off the northern Coast of Alaska. in: Reed, J.C., and Sater, J.E., eds. Beaufort Sea Coast and Shelf. pp. 439-476.
- Barnes, P.W., Reimnitz, E., Toimil, L., Maurer, D., and McDowell, D., 1979, Core Descriptions and Preliminary Observations of Vibracores From The Alaskan Beaufort Sea Shelf: U.S. Geologic Survey Open File Report 79-351 17pp.
- Billings, M.P., 1972, Structural Geology. Prentice-Hall Inc., Englewood Cliffs, New Jersey. pp. 35-94.
- Black, R.F. 1964, Gubick formation of Quaternary age in northern Alaska. U.S. Geological survey Professional paper 302-c 57-91pp.

- Carsola, A.J. 1954a, Microrelief on arctic sea floor: Bulletin of American Association of Petroleum Geologists, 38:1587-1601.
- Carter, L.D., 1983b, Cenozoic glacial and glaciomarine deposits of the central North Slope, Alaska, in Thorson, R.M., and Hamilton, T.D., eds., Glaciation in Alaska, Extended Abstracts from a workshop: Alaska Quaternary Center, University of Alaska Museum Occasional Paper No. 2, pp. 17-21.
- Carter, L.D., Brigham-Grette, J., and Hopkins, D.M., 1986, Late Cenozoic Marine Transgressions of the Alaskan Arctic Coastal Plain. in: J.A. Heginbottom and J.S. Vincent eds., Correlation of Quaternary Deposits and Events around the margin of the Beaufort Sea: Contributions from a joint Canadian-U.S. workshop 1984, Canadian Geologic Survey open file report 12-37 pp. 21-26.
- Clayton, L., Laird, W.M., Klassen, R.W., and Kupsch, W.O., 1965, Intersecting Minor Lineations on the Lake Agassiz Plain: Journal of Geology, v. 73, p.652-656.
- Clayton, L., Moran, S.R., and Bluemle, J.P., 1980, Explanatory Text to Accompany The Geologic Map Of North Dakota: Report Of Investigation No. 69 North Dakota Geologic Survey, 21pp.
- Colton, R.B., 1958, Note on the Intersecting Minor Ridges in the Lake Agassiz Basin, North Dakota: North Dakota Geological Survey Miscellaneous Series 10, pp. 74-77.
- Craig, J.D., Sherwood, K.W., and Johnson, P.P., 1985, Geologic Report For The Beaufort Sea Planning Area, Alaska: Regional Geology, Petroleum Geology, Environmental Geology: OCS Report MMS 85-0111, 192pp.
- Craig, J.D., and Thrasher, G.P., 1982, Environmental Geology of Harrison Bay Northern Alaska: U. S. Geologic Survey Open File Report 82-35, 25pp.
- Dillon, W.P., and Oldale, R.N., 1978, Late Quaternary Sea Level Curve: Reinterpretation based on glaciotectonic influence: Geology, v. 6, pp. 56-60.
- Dinter, D.A., 1982, Holocene Marine Sediments on the Middle and Outer Continental Shelf of the Beaufort Sea North of Alaska: Miscellaneous Investigation Series Map I-1182-B.

- Dredge, L.A., 1981, Relict Ice-Scour Marks and Late Phases of Lake Agassiz in Northernmost Manitoba: Canadian Journal of Earth Science, v. 19 pp. 1079-1087.
- Emery, K.O., 1949, "Topography and Sediments of the Arctic Basin", Jour. Geol., V. 57, No. 5., pp. 512-521.
- Eyles, N., and Clark, B.M., 1986, Significance of Hummocky and Swaley Cross-Stratification in Late Pleistocene Lacustrine Sediments of the Ontario Basin, Canada: Geology, v. 14, pp. 679-682.
- Fenton, M.M., Moran, S.R., Teller, J.T., and Clayton, L., 1983, Quaternary Stratigraphy and History in the Southern Part of the Lake Agassiz Basin: in Glacial Lake Agassiz: Teller, J.T., and Clayton, L., eds. Geological Association of Canada Special Paper 26, pp. 49-74.
- Gross, M.G., 1982, Oceanography: A View of the Earth. Prentice-Hall Inc. Englewood Cliffs, New Jersey, pp. 140-172.
- Horberg, L., 1951, Intersecting Minor Ridges and Periglacial Features in the Lake Agassiz Basin, North Dakota: Jour. Geology, v. 59, no. 1, pp. 1-18.
- Kempema, E.M., 1983, Ice Gouge Infilling and Shallow Shelf Deposits in Eastern Harrison Bay, Beaufort Sea, Alaska in National Oceanic and Atmospheric Administration, Boulder, Co. Environmental Assessment of the Alaskan Continental Shelf: Principal Investigators Reports. Year Ending March, 1983.
- Kovacs, A. 1972, Ice scoring marks floor of the arctic shelf. Oil and Gas Journal (October 23), pp.92-106.
- Kovacs, A. and Mellor, M., 1974, Sea Ice Morphology and Ice as a Geologic Agent in the southern Beaufort Sea, in, Reed, J.C., and Sater, J.E., eds., The Coast and Shelf of the Beaufort Sea, Arctic Institute of North America, pp. 113-163.
- Mollard, J.D., 1983, The Origin of Reticulate and Orbicular Patterns On The Floor of the Lake Agassiz Basin: in Glacial Lake Agassiz: Teller, J.T., and Clayton, L., eds. Geological Association of Canada Special Paper 26, pp. 355-374.
- Naidu, A.S., 1974, Sedimentation in the Beaufort Sea: a synthesis. In Marine Geology and Oceanography of the Arctic, Y. Herman (Ed.), Springer-Verlag, New York.
- Naidu, A.S., Burrell, D.C., and Hood, D.W., 1971,

Clay Mineral Composition and Geologic Significance of some Beaufort Sea Sediments: Jour. of Sed. Pet., v. 41 pp. 691-694.

- Naidu, A.S., and Mowatt, T.C., 1974, Aspects of Size Distributions Mineralogy, and Geochemistry of Detail and Adjacent Shallow Marine Sediments, north arctic Alaska. U.S. Coast Guard, Oceanographic Report Series.
- Naidu, A.S. and Sharma, G.D. 1972, Texture, Mineralogy and Chemistry of Arctic Ocean sediments. University of Alaska, Institute of Marine Science, Report No. R72-12, 31pp. in: U.S. Coast Gaurd, Oceanographic Report Series.
- Payne, T.G. and others. 1951, Geology of the arctic slope of Alaska. U.S. Geological Survey Oil and Gas Investigations Map O.M. 126.
- Pelletier, B.R. and Shearer, J.M. 1972. Sea bottom scouring in the Beaufort Sea of the Arctic Ocean. In Marine Geology and Geophysics, proceedings of 24th International Geological Congress, sect.8,pp.251-61.
- Reading, H.G., 1986, Sedimentary Environments and Facies, Second Edition: Blackwell Scientific Publications, Palo Alto, Ca.
- Reimnitz, E. and Barnes, P.w. 1974, Sea ice as a geological agent on the Beaufort Sea Shelf of Alaska. in: Reed, J.C., and Sater, J.E., eds. Beaufort Sea Coast and Shelf. pp. 301-353.
- Reimnitz, E. Barnes, P.W. and Alpha, T.R. 1973, Bottom features and processes related to drifting ice on the arctic shelf, Alaska. U.S. Geological Survey Miscellaneous Field Studies Map, MF-532.
- Reimnitz, E. Barnes, P.W., Forgatsch, T.C. and Rodiek, C.A. 1972, Influence of grounding ice on the arctic shelf, Alaska. Marine Geology, 13:323-34.
- Reimnitz, E. and Bruder, K.F. 1972, River discharge into an ice-covered ocean and related sediment dispersal, Beaufort Sea, coast of Alaska. Geological society of America Bulletin, 83:861-66.
- Reimnitz, E., Rodeick, C.A. and Wolf, S.C. 1974, Strudel scours: a unique arctic marine phenomenon. Journal of Sedimentary Petrology.
- Reimnitz, E., Toilmil, L.J., and Barnes, P.W., 1978, Arctic Continental Shelf Morphology Related to Sea Ice Zonation, Beaufort Sea, Alaska. Marine Geology

v. 28, pp. 179-210.

- Reimnitz, E., Wolf, S.C. and Rodeick, C.A. 1972, Preliminary interpretation of seismic profiles in the Prudhoe Bay area, Beaufort Sea, Alaska. U.S. Geological Survey Open File Report 548, 11pp.
- Reimnitz, E., Graves, S.M., and Barnes, P.W., in press, Beaufort Sea Coastal Erosion, Sediment Flux, Shoreline Evolution, and The Erosional Shelf Profile. 28 pp.
- Reineck, H.E., and Singh, I.B., 1980, Depositional Sedimentary Environments: Springer-Verlag, New York, N.Y.
- Rex, R.W., 1955. Microrelief produced by sea ice grounding in the Chukchi Sea near Barrow, Alaska. Arctic, 8:177-86.
- Stearns, C.W., Carroll, R.L., and Clark, T.H., 1979, Geological Evolution of North America: Third Edition Wiley and Sons, Inc, New York, N.Y..
- Tarr, R.S., 1897, The Arctic Sea Ice as a Geological Agent. American Journal of Science, V. 3, pp. 223-229.
- Tucker, M.E., 1981, Sedimentary Petrology An Introduction: Blackwell Scientific Publications, Halsted Press, New York, N.Y..
- Walker, H.J., 1973, The Colville River and Beaufort Sea: Some Interactions: in The Beaufort Sea Coast and Shelf: Reed, J.C., and Sater, J.E., eds. pp. 513-541.
- Walker, H.J., 1976, Depositional Environments in the Colville River Delta: in Symposium Proceedings: Recent and Ancient Sedimentary Environments in Alaska, Miller, T.P., ed. Alaska Geologic Society pp. C1-C22.
- Yorath, C.J., Shearer, J., and Havard, C.J., 1970, Seismic and Sediment Studies in the Beaufort Sea: Geological Survey of Canada Paper 71-1, Part A, pp. 242-244.